



HAL
open science

Palaeotsunami deposits at the Tiber River mouth (Ostia Antica, Italy): Do they really exist?

Hugo Delile, Ferréol Salomon

► To cite this version:

Hugo Delile, Ferréol Salomon. Palaeotsunami deposits at the Tiber River mouth (Ostia Antica, Italy): Do they really exist?. *Earth-Science Reviews*, 2020, 208, pp.103268. 10.1016/j.earscirev.2020.103268 . hal-03045769

HAL Id: hal-03045769

<https://hal.science/hal-03045769v1>

Submitted on 21 Sep 2022

HAL is a multi-disciplinary open access archive for the deposit and dissemination of scientific research documents, whether they are published or not. The documents may come from teaching and research institutions in France or abroad, or from public or private research centers.

L'archive ouverte pluridisciplinaire **HAL**, est destinée au dépôt et à la diffusion de documents scientifiques de niveau recherche, publiés ou non, émanant des établissements d'enseignement et de recherche français ou étrangers, des laboratoires publics ou privés.



Distributed under a Creative Commons Attribution - NonCommercial 4.0 International License

1 **Palaeotsunami deposits at the Tiber River mouth (Ostia Antica, Italy): do** 2 **they really exist?**

3 Hugo Delile^{1,2*}, Ferréol Salomon³

4 ¹INRAE, UR RiverLy, 5 rue de la Doua CS 20244, F-69625 Villeurbanne, France

5 ²CNRS UMR 5133 Archéorient, Maison de l'Orient et de la Méditerranée, Université de Lyon
6 2, 69365 Lyon Cedex 7, France

7 ³Centre National de la Recherche Scientifique / Université de Strasbourg, Laboratoire Image
8 Ville Environnement UMR 7362, 3 rue de l'Argonne, 67083 Strasbourg cedex, France

9 *Corresponding author

10 Contact details:

11 +33 (0)6 82 73 66 53

12 hugo.delile@inrae.fr

13 **Keywords:** palaeotsunamis, pluridisciplinary proxies, geoarchaeology, Mediterranean Sea,
14 Ostia, Tiber delta, coastal research, Pb palaeopollution

15 **Abstract**

16 In this paper, we test the recent hypothesis of the occurrence of five to seven tsunami
17 generations, that would have struck the ancient harbour basin of Ostia (Italy), and the lower
18 channel of the Tiber River during the last three millennia. Because these steady disaster
19 events would have deep implications on our knowledge of the history of Rome, we reviewed
20 the pluridisciplinary data available at the Tiber River mouth. Considering sedimentological,
21 geomorphological, micropalaeontological, geochemical, chronological and historical
22 evidence, there is no conclusive palaeoenvironmental evidence to suggest past tsunami
23 inundations near Ostia yet. River mouths are not the best contexts to identify tsunami
24 deposits. High fluvial and coastal mobility generated by regular floods and storms hardly
25 records single high-energy event (HEE) from a flood, a storm, or a tsunami. Sediments are

26 regularly reworked at the river mouth both in the river channel and on the close shoreface.
27 Mixed fluvial and marine influences and the seasonal formation of a salt wedge at the mouth
28 of the Tiber create specific estuarine assemblages for micro- and macrofauna. The layer called
29 High-Energy Event 1 (HEE-1) on the palaeo-shoreface close to the river mouth and HEE-4 / 5
30 in the point bars of the Tiber channel are most probably layers reworked several times by
31 fluvio-coastal events (storms and/or floods). HEE-3 sealing the Republican harbour of Ostia is
32 clearly related to flood deposits. Complementary analyses would be necessary to definitely
33 identify the origins of the HEE-2 and HEE-7 in the harbour, and HEE-6 in the palaeochannel
34 or floodplain. Based on the data available, we show how other processes than tsunami
35 inundations could be just as accountable for these coarse-grained sediment layers (storm
36 deposit, flood deposit, or riverbank deposit). This review puts into question the use of
37 pluridisciplinary proxies to identify palaeotsunami deposits. In addition, we demonstrate how
38 high Pb concentrations constitute a robust proxy to definitively refute the presence of
39 palaeotsunami deposits. As such, this study will be beneficial to a large community of
40 specialists in coastal research.

41

42 **1. Introduction**

43 Scientific interest in palaeotsunami research has increased since the 2004 Indian Ocean
44 Tsunami (2004 IOT) and the following similar disastrous hazards, like those of the 2011
45 Tohoku-oki Tsunami (2011 TOT) and more recently of 2018 Palu Tsunami (Indonesia), for
46 which human losses were huge. This has resulted in a large range of methods developed in
47 different disciplines to characterise and assess the effects of these kind of high-energy events
48 (HEEs) on past human societies, as well as their ability to deal with it (e.g., their vulnerability
49 and resilience). One of the best area to explore this specific short-lived human-environment
50 interaction is the Mediterranean due to its long urban history of occupation over the last

51 millennia and its intense seismic activity. In this regard, coastal geoarchaeology is involved in
52 tracking palaeotsunami impacts along Mediterranean shores, promoting interdisciplinary
53 approaches including sedimentology, geomorphology, micropalaeontology, geochemistry,
54 archaeology, and history. Among the sites and stratigraphic tsunami deposits documented all
55 around the Mediterranean (e.g., Maramai et al., 2014; Reicherter et al., 2019; Marriner et al.,
56 2017), one of them involves the iconic city of ancient Rome. Because tsunami inundations
57 would not be without significant impacts on our understanding of the history of Ancient
58 Rome, we have paid a special concern to them.

59

60 During the last ten years, several geoarchaeological research were conducted in the area
61 of the archaeological site of Ostia, the ancient port of Rome at the mouth of the Tiber River.
62 Two research teams applied similar or complementary methods to analyse and interpret
63 fluvio-coastal dynamics dating from the Roman period.

64 In the early 2010's, Goiran et al. (2012, 2014) published definitive chronostratigraphical
65 and palaeoenvironmental evidence for the location of the harbour of Ostia (Fig. 1). Later,
66 complementary analyses were conducted on these cores (Goiran et al., 2012, 2014, 2017;
67 Sadori et al., 2016; Salomon et al., 2016; Delile et al., 2017, 2018), while the second team
68 conducted more extended surveys in the area involving complementary cores and geophysical
69 surveys (Hadler et al., 2015; Wunderlich et al., 2018; Vött et al., 2015, 2020). In parallel,
70 geoarchaeological research was conducted in the palaeomeander of Ostia that was flowing in
71 the city of Ostia during the Roman period. The first team conducted studies in the area of the
72 *Castello Giulio II* and in the area of the *Castrum* of Ostia (Salomon 2013; Pepe, et al., 2016;
73 Salomon et al. 2017, 2018), although the second team studied two cross-sections of the
74 palaeomeander of Ostia between these two locations (Wunderlich et al., 2018; Hadler et al.,
75 2020).

76 The presence of these two teams contributed to produce a lot of essential new data to
77 reconstruct the evolution of the landscape of this important city-port from the Roman period.
78 However, the two teams propose different interpretations of the deposits. On the basis of
79 geomorphological, sedimentological, geochemical, geophysical and microfossil analyses,
80 Hadler et al., (2015, 2020), Wunderlich et al. (2018) and Vött et al. (2020) hypothesize the
81 existence of seven palaeotsunami deposits (High Energy Event 1 to 7 spelled thereafter HEE-
82 1 to 7) attributed to five to seven different events (Table 1). Amongst these tsunami events,
83 three to four would have hit the active port-city of Ostia during the Roman period. In contrast,
84 none of these deposits were interpreted such as tsunami by the other team (Goiran et al., 2012,
85 2014, 2017; Sadori et al., 2016; Pepe et al., 2016; Salomon et al., 2016, 2017, 2018; Delile et
86 al., 2017, 2018).

87 For this reason, it seems crucial to test these palaeotsunami hypotheses by focusing on
88 all pluridisciplinary data available at the mouth of the Tiber River. This paper reviews
89 sedimentological, geomorphological, micropalaeontological, geochemical, archaeological,
90 chronological, and historical accounts that were gathered these last years on the study area.
91 This study is based on (i) a re-examination of evidence published in Hadler et al. (2015 and
92 2020) and Vött et al. (2020), together with other palaeoenvironmental data from other cores
93 drilled in the area (Goiran et al., 2014; Sadori et al., 2016; Salomon et al., 2016, 2017; Delile
94 et al., 2017, 2018), (ii) a discussion of a complementary approach using lead (Pb)
95 concentrations as a reliable exclusion indicator of the extreme wave event hypothesis, and (iii)
96 a critical comment on the chronology proposed by Hadler et al. (2015, 2020) and Wunderlich
97 et al. (2018), based on radiocarbon dates. Finally, this work highlights pitfalls that should be
98 avoided while identifying palaeotsunami deposits in fluvio-coastal environments, including
99 ancient harbours.

101 **2. Sedimentary features**

102 Usually, the first evidence suggesting a palaeotsunami deposit within a stratigraphy is
103 the presence of a coarse-grained layer trapped in finer deposits, which are separated by a basal
104 erosional surface at the base of the palaeotsunami deposit (Dawson et al., 1988 ; Morton et al.,
105 2007 ; Engel and Brückner, 2011 ; Shanmugam, 2012 ; Rubin et al., 2017 ; Röbbke and Vött,
106 2017). Ideally, low energy palaeoenvironments such as lagoons, coastal freshwater lakes, and
107 mangroves, are the most appropriate places in which to identify palaeotsunamis deposits. In
108 such contexts, HEEs are expressed by a short-time disturbance in the ambient low-energy
109 milieu. Theoretically, if the protected palaeoenvironment is away from direct fluvial or
110 coastal influence, it limits the number of natural processes that are able to settle into distinct
111 coarse layers. A compilation of different sedimentological signatures (presence of rip-up
112 clasts, fining upward sequence, mud cap, reworked underlying sediment, basal load structure),
113 together with palaeoenvironmental indicators (palaeoecological markers, geochemical
114 signatures) have to be considered before suggesting any interpretations. All of this evidence
115 will be reviewed in this paper.

116 The first high-energy event (HEE-1) identified by Hadler et al. (2015) was observed in a
117 pre-harbour deposit around 6 m below sea level (b.s.l.) (6.36 to 5.61 m b.s.l.) in Core OST-3
118 (HEE-1 - Fig. 2 and Table 1). The environmental context (shallow marine environment with
119 fluvial influence, shoreface) is dated to at least to the 9th - 8th c. BC in Core OST-1 at 8.81m
120 b.s.l. and before the 4th c. BC (oldest radiocarbon dates for the establishment of the harbour of
121 Ostia). A coarse-grain layer is observed in Core OST-3, together with a basal erosional
122 surface, a fining upward sequence with a mud cap, rip-up clasts, and gravels (Table 1). For
123 this first event, all sedimentological indicators observed could support the tsunami hypothesis,
124 but do not exclude flood or storm hypotheses. Along with Goiran et al. (2012, 2014) and
125 Sadori et al. (2016), we insist on the depositional context. All research teams agreed on the

126 existence of a shallow marine / shoreface environment with fluvial influence from the river
127 mouth near Ostia in this area at the beginning of the 1st millennium BC (Goiran et al., 2014;
128 Hadler et al., 2015; Sadori et al., 2016; Delile et al., 2018; Salomon et al., 2018). The Tiber
129 delta is a wave-dominated delta. However, at the scale of the river mouth, the promontory
130 alternate between river and wave dominated morphologies. River mouth environments are
131 known to be fast changing environments. River mouth bars form and change regularly. Sandy
132 shoreface morphologies close to a river mouth are highly mobile and constantly exposed to
133 floods and storms. Additionally, it has been demonstrated that the Tiber River mouth was
134 particularly dynamic during the first part of the 1st millennium BC: quick progradation
135 shaping a large promontory and river channel migrating toward the south (Bellotti et al.,
136 2011; Milli et al., 2013; Delile et al., 2018; Salomon et al., 2018; Salomon, 2020).

137 Hadler et al. (2015) hypothesise that “fluvial sediments were dislocated by a high-
138 energy event within a near-shore deltaic marine environment”, and attest to the difficulty in
139 identifying the fluvial and coastal balance in such environments. Since the sedimentological
140 signature of this deposit could also be attributed to a fluvial or a storm event, we suggest
141 leaving all interpretations open to the origin of this HEE-1. No sedimentological evidence
142 alone should definitively proves a paleo-tsunami signature. Alternatively, we would suggest
143 that the layer identified could be related to through/bar deposits near the palaeoriver mouth of
144 the Tiber River (Salomon, 2013, 2020). Deposits similar to HEE-1 can be identified in almost
145 all cores drilled between Ostia and Fiumicino in depths ranging between 4 to 9 m below the
146 current sea level and related to different progradational phases (Salomon, 2013). These layers
147 offer badly sorted silty sand with some little gravels, cross-bedded structure often trapping
148 organic layers, and the D50 is systematically finer than 200 µm below this layer and coarser
149 than 200 µm above the same layer. Current D50 distribution along the coasts of the Tiber
150 delta demonstrates similar grain-size pattern associated to the lower, middle (breaker zone,

151 longshore bars), and upper shoreface (Noli et al. 1996; Tortora, 1999; Tentori et al., 2018). In
152 this interpretation, several events, several seasons and longer-term evolution would have
153 occurred to form HEE-1 layer involving fluvial inputs (floods) and coastal reworking (mainly
154 littoral drift and storms). Afterward the progradation of the Tiber River mouth definitely
155 trapped these reworked shoreface deposits. A tsunami could have happened, but its imprint
156 would not be properly distinguishable amongst other processes involved in the marine side of
157 the palaeo-river mouth.

158 In the harbour of Ostia, three coarse sandy layers were assigned to palaeotsunami
159 events: HEE-2 (3.28-3.05 m b.s.l.), HEE-3 (1.45-0.12 m b.s.l.), and HEE-7 (0.65-0.15 m
160 b.s.l.) (see Fig. 2 for Core OST-3; complementary information from Core PO-2 in the Fig. 3
161 in which the gray bands refers to the high siliciclastic inputs associated to the palaeotsunami
162 events HEE-1, HEE-3 and HEE-7; and Table 1). Generally, enclosed harbour environments
163 are good traps for palaeotsunami deposits. HEE-2 and -3 layers clearly expose a change in the
164 facies with increasing grain-size, the presence of basal unconformities, and rip up clasts, but
165 no clear mud caps. However, no specific grain-size grading is observed. Unfortunately, in the
166 light of the above mentioned, we cannot definitively exclude marine strong storms and fluvial
167 major floods as potential sources of these coarse layers, since these processes could imply
168 sedimentological characteristics similar to tsunamites. In our opinion, the hypothesis of a
169 storm reaching the harbour cannot be totally excluded considering current strong storms (Noli
170 et al., 1996), and the geography of Ostia during the Roman period. According to the
171 palaeogeographical reconstructions, the mouth of the Tiber River was ca. 200 m to the north-
172 west and the coastline ca. 200m to the south in the second part of the 1st millennium BC and
173 the beginning of the 1st millennium AD (Salomon et al., 2018) (Fig. 1).

174 The HEE-7 layer is located in the area of the ancient harbour of Ostia, in a chamber of
175 the shipshed (or navalia-temple complex) with pillars built in the 2nd c. AD (Vött et al. 2020;

176 Heinzlmann, 2020). HEE-7 layer (Fig. 4 and Table 1) demonstrates a change in the facies
177 with a normal grading. However, the absence of a basal erosional surface and rip up clasts,
178 and no clear mud caps do not argue in favour of a palaeotsunami deposit. This sandy deposit
179 is located within the range of the relative ancient sea levels identified in Ostia and Portus
180 (Goiran et al. 2009; Heinzlmann, 2020). The context and the facies of the sediment could
181 suggest a deposit related to a sandy riverbank of the Tiber close to the river mouth and semi-
182 sheltered in the shipshed building.

183 The harbour basin of Ostia was located close to the river mouth. Consequently, the
184 action of fluvial and marine processes makes the identification of tsunami deposits more
185 complex.

186

187 Finally, three deposits were considered most likely from palaeotsunami origin in the
188 palaeomeander of Ostia – HEE-4/5 in Core TEV-4A and HEE-6 in Core TEV-1A (Hadler et
189 al., 2020) (Figs. 5 and 6, and Table 1). The precise depths of the HEEs are not reported in the
190 original publication, but their estimates were reported in the figures 5 and 6. Again in this
191 context, no clear sedimentological evidence supports the tsunami hypothesis. All of the HEE
192 deposits observed in Core TEV-4A were identified during the period of activity of the
193 palaeochannel. In such environments, the preservation of tsunami deposits is poor due to high
194 post-depositional disturbances derived from fluvial processes. In this respect, an active
195 riverbed is regularly re-shaped according to events (floods), or season (flood period).
196 Additionally, based on the data provided by Hadler et al. (2020), there are no changes in the
197 facies, no basal erosional surface, no visible rip-up clasts, no normal grading and no mud cap.
198 In this highly dynamic fluvial dynamic environment, grain-size is considerably changing and
199 no clear event can be identified for palaeotsunami deposits (Figs. 5 and 6, and Table 1).

200 The high-energy event identified in Core TEV-1A (HEE-6) was dated to a later period
201 (Table 1), and trapped in floodplain deposits on top of the infilled palaeochannel formed after
202 the cut-off started in 1557. It is a better context in which to look for tsunamites. However,
203 Hadler et al. (2020) do not describe any sedimentological marker suggesting a palaeotsunami
204 deposit. Grain-size change seems progressive more than abrupt, and the facies is rather
205 homogeneous. Based on these observations, we would interpret the progressive increase and
206 decrease of the grain-size, such as a manifestation of a period of higher flood activity.

207 In general, the facies of the three high-energy events identified in the palaeochannel of
208 Ostia are similar to their depositional context (see photos in Figs. 4 and 5 from Hadler et al.,
209 2020). The identification of the HEEs is based on single analysed samples (TEV4A/11 for
210 HEE-4; TEV4A/4 for HEE-5; and Sample TEV1/9 for HEE-6) and rely mainly on
211 foraminifers.

212 To conclude this part on sedimentological evidence, storms or floods along with
213 palaeotsunami origins should still be considered as valid hypotheses for the deposits identified
214 in the harbour of Ostia (HEE-2, -3 and -7) and in the 1st millennium BC shoreface close to the
215 palaeoriver mouth (HEE-1) (Hadler et al., 2015). However, the sedimentary facies of HEE-3
216 is similar to a fluvial bedload-derived deposit identified in the palaeomeander of Ostia
217 (Salomon et al., 2017) and the canals of Portus (Salomon et al., 2014).

218 In the palaeomeander of Ostia, no sedimentological evidence supports the hypothesis of
219 a palaeotsunami (Hadler et al., 2020). Complementary indicators are discussed here below.

220

221 **3. Geomorphological features**

222 One of the most used geomorphological fingerprints of tsunamites in the literature
223 concern the fining-landward sequence (e.g., Goff et al., 2001 ; Paris et al., 2007 ; Engel and

224 Brückner, 2011 ; Röbbke and Vött, 2017), and the great spatial distribution of these deposits
225 (e.g., Morton et al., 2007; Pignatelli et al., 2009; Marriner et al., 2017).

226 We should first observe that the distribution of the sedimentary cores is not appropriate
227 to look at this evidence, especially in an urbanised river mouth such as Ostia. The diversity in
228 the palaeoenvironments and the complexity of the topography in a city would clearly affect
229 the distribution of the deposits and their preservation. As a result, thickness correlations
230 between the HEEs identified in the harbour of Ostia and the palaeochannel of Ostia would be
231 hazardous, since there are completely different depositional contexts.

232 In accordance with Hadler et al. (2015), only HEE-3 deposit will be discussed in this
233 section (Fig. 2 and 3): the upper thick high-energy event deposit was recorded in the whole
234 harbour of Ostia by all research teams. In contrast, HEE-2 trapped in the harbour (e.g.,
235 observed in Core PO-1 and OST-3, but not in PO-2 and OST-5, OST-8) was not observed in
236 all the cores.

237 HEE-7 is for now only restricted to the area of the shipshed chambers. According to Vött et
238 al. (2020) “this event is interpreted as a tsunami that hit the wider coastal region”. However,
239 for now, Tyrrhenian coasts do not provide any evidence of the spatial expansion of this
240 youngest tsunamite recorded into the harbour basin.

241 In the harbour of Ostia, while it was argued that the “thinning landward and uphill”
242 criterion is fulfilled for the HEE-3 deposit recorded at Ostia, the NW-SE oriented-cross-
243 section provided by Hadler et al. (2015) is roughly perpendicular to the Tiber palaeochannel
244 and toward uphill, but not perpendicular to the coastline (Fig. 1). The first cross-section
245 displays cores OST 8, 3, 5 and 4 with an associated-event HEE-3 thickness of about ~ 1.5 m,
246 1.5 m, 2 m and 1.5 m, respectively. These values are therefore indicative of a regular
247 thickness of the high-energy event deposit, but do not express a landward fining sequence.

248 Thickness of the layers would have made sense in a wider spatial context with more regular
249 topography.

250

251 **4. Micro-faunal features**

252 The hypothesis of the occurrence of seven tsunamis deposits at Ostia is mainly
253 supported by the foraminifera contents in Hadler et al. (2015, 2020) and Vött et al. (2020),
254 which are known to contribute to the identification of such events (Hawkes et al., 2007).
255 However, bioindicators should be interpreted carefully since there is no absolute evidence
256 using foraminifers that attests to tsunami origin of deposits (Mamo et al., 2009).

257 Considerations reported here are based on the data provided by Hadler et al. (2015,
258 2020) and Vött et al. (2020). In Figures 2, 4, 5 and 6, only few parameters related to
259 foraminifers are reported. For the full tables of foraminifers, we refer to the original
260 publications.

261

262 **4.1. Indigenous and autochthonous foraminifers at the mouth of the Tiber River**

263 The clear attribution of a coarse deposit to a tsunami using foraminifers usually needs
264 the presence of deep water assemblages (pelagic and/or benthic species and/or deep water
265 species) in coastal environments (shallow water, brackish) and/or, to a lesser extent, a sudden
266 change in the assemblage, and a higher species diversity (Dawson et al., 1995; Hindson and
267 Andrade, 1999; Hindson et al., 1996, 1998; Hawkes et al., 2007; Mamo et al., 2009). For the
268 Tiber delta, this would be finding offshore foraminifers assemblages (Di Bella et al., 2013) in
269 the coastal area. Additionally, taphonomic characters, breakage of tests, nature and
270 importance of the abrasion should be considered.

271 According to the synthesis produced by Mamo et al. (2009), “it seems to be easier to
272 distinguish displaced ”open” or “fully marine” assemblages within a marsh setting than it is to

273 distinguish a displaced marine assemblage in an estuarine or lagoonal setting”. Considering
274 the palaeoriver mouth of Ostia, the depositional contexts (shoreface, harbour and river
275 channel all close to the palaeo-river mouth of the Tiber) are definitely not ideal to identify a
276 clear assemblage suggesting a tsunami (Table 1).

277

278 In its lower reach, the Tiber River built a delta with accumulation of fluvial sediments
279 partially reworked by the sea (Bellotti et al., 2007; Milli et al., 2013). However, the river
280 mouth channels offers an ecological context similar to estuaries (Mikhailova et al., 1999;
281 Capelli and Mazza, 2008; Manca et al., 2014). A salt water wedge forms seasonally in the
282 delta and the maximum of sea water intrusion can penetrate at least ca. 9 km inland
283 (Mikhailova et al., 1999). The Tiber delta is formed in a microtidal area, and the more
284 probable cause of salt wedge intrusion might be the wind action (Manca et al., 2014).

285 Consequently, *autochthonous foraminifers* can develop within the lower course of the
286 Tiber River similarly to other estuarine environments (Wang, 1992; Wang and Chappell,
287 2001; Ruiz et al., 2005). This estuarine context can explain the presence of marine
288 foraminifers in a good state of preservation recorded within the ancient harbour of Ostia or in
289 the palaeochannel (see below).

290 Additionally, in accordance with Hadler et al. (2015), it should also be reminded that
291 *allochthonous foraminifers* can derive from the erosion of recent or much older deposits.
292 *Globigerinoidae* are the most represented in the core OST-3 (harbour of Ostia), and “most
293 likely derives from the local bedrock within the hinterland of the Tiber River (Bellotti et al.,
294 2007)” (Hadler et al. 2015).

295

296 **4.2. Estuarine environments observed in the palaeoriver mouth**

297 In Core OST-3, the most obvious change of assemblage occurs from the pre-harbour to
298 the harbour environment. Pre-harbour shoreface / river mouth deposits display a large range
299 of foraminifers developing in marine to shallow marine environments in important quantities
300 (Fig. 2). Except for the allochthonous planktonic foraminifers, *Ammonia beccarii*,
301 *Cassidulina* spp., *Nonion* sp., *Ammonia tepida* and *Trioculina* sp. are the most frequent taxa.
302 In contrast, less species and less quantities of foraminifers are recorded in the harbour
303 deposits (Fig. 2). *Ammonia beccarii*, *Cassidulina* sp., and *Bolivina* sp. are the most
304 represented taxa in the harbour. Interestingly, between the river mouth shoreface
305 environments and the harbour of Ostia, the diversity of foraminiferal species decreases, but
306 most of the species in the harbour are also present in the pre-harbour deposit. Only *Adelosina*
307 sp. and *Eponides* sp. are observed in the harbour, but their quantity is not representative.
308 Accompanying taxa of *Ammonia tepida* and *Trioculina* sp. seem to characterise more the
309 shoreface / river mouth environment in OST-3, while *Bolivina* sp. is more present in the
310 harbour. However, *Ammonia* sp. and especially *Ammonia beccarii* are highly represented in
311 all the stratigraphies studied. The fluvio-coastal stratigraphy from Core OST-7A is only of 2
312 m (Vött et al., 2020) (Fig. 4) and it should have been compared with other cores. HEE-7
313 (Units VII and VIII in Core OST-7A in Vött et al., 2020) demonstrates a clear increase in the
314 quantity and the diversity of foraminifers. However, there is no clear shift of the assemblage.
315 *Ammonia* sp. is still highly represented along with *Cassidulina* sp., *Cibicidoides* sp., *Bulimina*
316 sp., *Nonion* sp., but also *Haynesina* sp. This layer can be related to another variation of the
317 estuarine environments of the Tiber River mouth.

318 The foraminiferal assemblage of the palaeomeander of Ostia (Cores TEV-4A and TEV-
319 1A) (Figs. 4 and 5) is largely similar to the ones observed on the shoreface / river mouth and
320 the harbour. *Ammonia beccarii*, *Cibicidoides pseudoungerinus* (*Cibicidoides*
321 *pseudoungeriana*?), *Cassidulina* spp. are the most represented (again excepting reworked

322 *Globigerinoidae*). *Cibicidoides pseudoungerinus* are more representative in the depositional
323 environment of the palaeochannel, but *Cibicidoides* sp. were largely observed in the coastal
324 river mouth environments in Core OST-3 and in HEE-3 trapped in the harbour of Ostia.
325 Accompanying taxa such as *Melonis barleeaanum*, *Pullenia* spp., *Bulimina* spp., *Cibicides*
326 *refuigens*, *Quinqueloculina seminula* are also more specific of the palaeochannel
327 environments.

328 Diversity between foraminifer assemblages expresses different estuarine conditions.
329 The different assemblages observed at the mouth of the Tiber River display some differences
330 but overall, all ecological contexts are related to estuarine environments. Except
331 allochthonous foraminifers, *Ammonia* sp. / *Ammonia beccarii* are the dominant taxa/specie
332 observed in all depositional contexts, and are characteristic of estuarine environments (Wang,
333 1992; Wang and Chappell, 2001; Ruiz et al., 2005; Di Bella et al., 2011). The common
334 presence of *Haynesina* sp. (characteristic of brackish environments) in all environments
335 suggest the same conclusion. It confirms that the coastal river mouth, the harbour, and the
336 palaeochannel of Ostia all express fluctuations of the estuarine environments of the Tiber
337 River (Fig. 2, 4 and 5).

338

339 **4.3. What are the foraminiferal characteristics of the high-energy events?**

340 In our opinion, for each of these high-energy layers identified around Ostia, the
341 foraminifers never display deep water assemblage inputs and/or sudden displaced
342 assemblages suggesting a palaeotsunami deposit. Also, no discriminant species specifically
343 characterise the seven high-energy events from their context.

344 HEE-1 in Core OST-3 demonstrates a sharp quantitative change expressed by a lower
345 quantity of foraminifers on the shoreface / river mouth (Fig. 2). The diversity of species is
346 very low considering each three samples picked in the HEE-1 by Hadler et al. (2015) (11 to

347 15 species). However, no distinct assemblage characterises HEE-1 (Fig. 2). In consequence,
348 these evidence could support the hypothesis of fluvial sediments reworked by coastal
349 processes (Hadler et al. 2015), and the hypothesis of a river mouth to coastal though/bar
350 context (Salomon, 2013). However, we consider that a distinct deposit attributed to a single
351 flood, a single storm or a potential tsunami would be unlikely (Table 1).

352 The pattern is different for the two upper high-energy events (HEE-2 and 3) recorded in
353 the harbour (Fig. 2). A rise in quantity and diversity comparing to the average harbour
354 environments (HEE-2 = 16; HEE-3 = 18) can be observed. However, the assemblage is not
355 distinct from the other estuarine environments of the area of Ostia – *Ammonia sp.* or *Ammonia*
356 *beccarii* are still dominant and accompanied with *Cassidulina sp.* Additionally, the quantity
357 of foraminifers never reaches abundant quantities (except allochthonous planktonic taxa)
358 (according to the semi-quantitative data from Hadler et al. 2015). It should be noted that
359 between HEE-2 and 3, two samples in Units IVb display the presence of 15 different species
360 recorded in silt and clay deposits, also with a similar assemblage (Hadler et al. 2015). Since
361 there are no coarser sediment, there are not a high-energy events. Few to common quantities
362 are also observed, similar to HEE-2 and 3 (Hadler et al. 2015). Again, in our opinion, this
363 demonstrates the complexity of the estuarine environments affected by the salt water wedge.

364 A shift in quantity and diversity is observed in HEE-7 in regards to the 2-meter
365 stratigraphy from Core OST-7A (Fig. 4), but with no specific assemblage considering all
366 cores (OST-3, TEV-1A, TEV-4A). According to Vött et al. (2020), species and taxa of
367 “*Ammonia beccarii*, *Neoconorbina sp.*, *Nodosaria sp.*, *Nonion sp.*, *Rosalina sp.*, *Valvuleria*
368 *sp.*” (error - *Valvulineria sp.*?) seems to be almost exclusively found in HEE-7. However,
369 similar foraminifers are found also in important proportions in the lower part of Core OST-7A
370 (abundant and dominating *Cassidulina sp.*, *Ammonia sp.*, *Nonion sp.*). Additionally, these
371 taxa and species are also found in other estuarine environments in cores OST-3, TEV-4A, and

372 TEV-1A. *Neoconorbina sp.*, *Nodosaria sp.* are present but remain low in all samples analysed
373 in these cores including in HEE-7. *Rosalina sp.* seems to be the only outlier of HEE-7 in the
374 context of all the cores analysed in the Tiber River mouth. However, it is not sufficient to
375 define a shift in the assemblage. Since HEE-7 is located close to the Roman relative sea levels
376 (Goiran et al. 2009 or Heinzelmann, 2020), we suggest to consider floating and swashing on
377 the riverbank such as important factors that would have enriched this unit in foraminifers.
378 These hypotheses should be tested.

379 In Core TEV-4A, HEE-4 and HEE-5 do not display the most species diversity of
380 foraminifers nor the lowest (Fig. 6) (Hadler et al., 2020). Additionally, changes related to
381 foraminifers are rather progressive and do not demonstrate abrupt events. Surprisingly, fluvial
382 deposits (even in bedload-derived deposits) trapped many foraminifers of different species in
383 the stratigraphies. Even more surprising, after Hadler et al. (2020), these foraminifers are in a
384 good state of preservation. This suggests that in the lower reach of the Tiber River the
385 presence of foraminifers in coarse sediment is not a good indicator for distinguishing marine
386 or fluvial high-energy events.

387 Again, in Core TEV-4A, there is no assemblage of foraminifers specific to the
388 suggested high-energy events compared to the depositional environments of the
389 palaeochannel of Ostia. The most represented taxa are *Ammonia Beccarii*, *Cassidulina* spp.,
390 *Cibicidoides pseudoungerinus* (except allochthonous taxa) accompanied by *Melonis*
391 *barleeanum*, *Pullenia* spp., *Bulimina* spp., *Cibicides refuigens*, *Quinqueloculina seminula*
392 (Hadler et al., 2020). They are also the most common within the full sequence of Core TEV-
393 4A (Fig. 6). In our opinion, the intrusion of the salt wedge controls the developments of
394 foraminifers within the channel (see above).

395 Interestingly, Hadler et al. (2020) observe “some juvenile articulated specimens of the
396 marine bivalve *Lentidium mediterraneum*” and “(articulated) brackish ostracods” in Sample

397 TEV 4A/11, i.e., in the sample interpreted such as the HEE-4. They suggest that it is
398 “associated with shallow water and frequently occurring in sandy estuarine environments”
399 (Hadler et al., 2020), which corroborate the estuarine interpretation of these foraminifers
400 (Wang, 1992; Wang and Chappell, 2001; Ruiz et al., 2005). In this regards, Hadler et al.
401 (2020) observe “the foraminiferal content of deposits from high-energy environments
402 frequently decreases with increasing grain size and is mostly restricted to few large, abraded
403 individuals, clearly reflecting assemblages disturbed by strong flow dynamics”. This remark
404 matches the hypothesis of autochthonous foraminifers developed within the river channel
405 when energy is lower. Combining the foraminiferal data (no specific assemblage, no specific
406 increase or decrease in quantity) and the sedimentological data (“macroscopically no changes
407 were observed for the respective events” - Hadler et al., 2020, - with no particular grain-size
408 coarsening) (Table 1), identifying tsunami or storm deposits in the active river channel in
409 Ostia seems unlikely.

410 Finally, the influence of the salt wedge cannot affect Core TEV-1A / Unit D (Fig. 5)
411 since the depositional context might have been already disconnected from the river and the
412 sea when the HEE-6 occurred. In TEV-1A, Unit D is interpreted as a floodplain deposit.
413 Considering (i) the homogeneity of the facies of Unit D, (ii) the gradual increase and decrease
414 of grain-size in Unit D, (iii) the presence of *Cassidulina* spp., *Cibicidoides pseudoungerinus*,
415 *Ammonia Beccarii* also dominant in TEV-4A (estuarine markers), and (iv) the occurrence of
416 all these foraminifers in Unit D (common to very common), we would interpret Unit D such
417 as an increase/decrease of flood activity during the last centuries with a peak in HEE-6 (Table
418 1). In this scenario, well preserved foraminifers would have been transported by floods. Since
419 we observe a certain amount of foraminifers (common) in all floodplain deposits analysed in
420 Unit D, this hypothesis is not impossible. However, it should be explored in more details.

421

422 **4.4. Conclusive remarks about the foraminifers at the mouth of the palaeo-Tiber River**

423 The reinterpretation of the foraminiferal data provided in Hadler et al. 2015 and 2020
424 and in Vött et al. (2020) suggests no clear evidence for a single marine HEE such as a tsunami
425 around Ostia. This reinterpretation applies to a major tsunami, which should have been clearly
426 marked by the foraminiferal assemblage, and to a minor tsunami, which is even more difficult
427 to track in estuarine environments. In our opinion, all the cores (OST-3, OST-7A, TEV-4A,
428 TEV-1A) display different expressions of the estuarine environment. The development of
429 autochthonous foraminifers in the river mouth environments of the Tiber, their reworking and
430 transport during floods, and the floating and the swashing of some species on the riverbanks
431 should be considered seriously and tested. More precise species identification of foraminifers
432 would help to better characterise the depositional environments and interpret the HEE
433 identified. Additionally, statistical treatments would be helpful to bring more information
434 about the foraminiferal assemblages and the depositional contexts - freshwater influence,
435 organic matter content (like in the publication of Di Bella et al. (2011) for the harbour of
436 Portus located a few kilometers in the north).

437 Determination of fluvial / marine origins of the HEE deposits should also be tested
438 against geochemical evidence.

439

440 **5. Geochemical evidence**

441 As reported by the number of publications related to tsunami and chemistry since 2005
442 (Chagué-Goff et al., 2017), the use of geochemical proxies in the tsunami research field has
443 evolved exponentially over the past few years. This trend is explained both by recent
444 devastating tsunamis (e.g., 2004 Indian Ocean Tsunami (2004 IOT), 2011 Tohoku-oki
445 Tsunami (2011 TOT), and 2018 Palu Tsunami), and by the increasingly recognized value of
446 this powerful tool for the identification of historical and/or prehistorical deposits (Chagué-

447 Goff et al., 2017; Röbbke and Vött, 2017). In this section, we will explain how elemental
448 geochemistry and Pb isotopes in sediments provide substantial value in the debate related to
449 the record or absence of multiple palaeotsunami deposits in the ancient harbour basin of Ostia.

450

451 **5.1. Elementary geochemistry**

452 Recently, the elemental geochemistry of siliciclastic deposits of Ostia's harbour basin
453 has been documented by measuring the concentrations of 39 chemical elements on 86 samples
454 regularly distributed in the harbour stratigraphy. In order to explore the thousands of data, a
455 Factor Analysis was performed, which is a statistical treatment consisting of converting data
456 into uncorrelated and limited variables known as factors (Fig. 3) (Delile et al., 2018). This
457 approach combining geochemistry and statistics was recently discussed to identify tsunami
458 deposits based on specifically saltwater inputs indicators (Chagué-Goff et al., 2017). Amongst
459 them, Na is considered a sensitive chemical proxy to identify palaeotsunami deposits
460 (Shanmugam, 2012 ; Chagué-Goff et al., 2017; Röbbke and Vött, 2017).

461 The results obtained by the mean of this method at Ostia (Fig. 3) identifies
462 environmental factors leading to the formation of the harbour basin deposits. In order of
463 importance these factors are (in %) (Delile et al., 2018): (i) the velocity of currents (the
464 siliciclastic terrigenous signal ~ 47%), (ii) the low hydrodynamics conditions (the
465 aluminosilicates signal ~ 13%), (iii) the harbour water column ventilation (the authigenic
466 fluxes ~ 10%), (iv) the seawater vs. freshwater influence (~ 7%). Factors 1 and 4 are
467 particularly relevant to recognize palaeotsunamis deposits because they trace the ambient
468 hydrodynamics and the river/marine origin of the currents, respectively. The red bands in
469 Figure 3B (Units A, B2 and C) indicate the sedimentary deposits interpreted as tsunamis-
470 related HEE-1 and 3 by Hadler et al. (2015).

471 Negative values of F1 (in blue) in Figure 3B confirm strong currents involved in HEE-1
472 and 3, but not in HEE-2 (positive values of F1 in red). For HEE-1 recorded in the upper part
473 of Unit A, the marine origin of the water is demonstrated by the positive values (in red) of F4
474 (Fig. 3B), which is used to support a tsunamigenic origin (or strong storm) in this unit.
475 However, the dramatic oxygen depletion (tsunami or storm events imply well oxygenated
476 water column) (see negative values in blue of F3 in Fig. 3B), and the over-representation of
477 estuarine lagoonal ostracod groups (Goiran et al., 2014 ; Sadori et al., 2016; Delile et al.,
478 2018) do not support the tsunamigenic hypothesis. Unit A displays all characteristics of a
479 classic pre-harbour deposit typical of a deltaic front sequence, which is widely documented at
480 the scales of the site itself, as well as the Tiber delta as a whole (Mazzini et al., 2011; Goiran
481 et al., 2012 ; 2014 ; Salomon, 2013 ; Salomon et al., 2012, 2018 ; Delile et al., 2014 ; Delile et
482 al., 2014a,b, 2018 ; Sadori et al., 2016).

483 The second coarse Unit B2 of Core PO-2 corresponds to the HEE-3 inferred from the
484 study of Hadler et al. (2015). The Factor Analysis of the geochemical signal suggests strong
485 currents (see negative values in blue of F1) from fluvial origin (see negative values in blue of
486 F4) (Fig. 3B). This freshwater signal in the harbour basin is the strongest recorded in the
487 stratigraphy. Unit B2 records the peak of a dynamic initiated in Unit B1a (Fig. 3B). This
488 gradual and continuous regression of seawater in favor of freshwater influence recorded in the
489 harbour stratigraphy is visible with Factor 4 (Fig. 3B).

490

491 **5.2. Trace metal palaeopollutions: a powerful tool to identify palaeotsunami deposits**

492 *5.2.1. Conceptual model of the trace metal palaeopollutions recorded before, during, and* 493 *after a palaeotsunami into the sedimentary archives of ancient harbour basins*

494 According to Hadler et al. (2013), allochthonous materials composing of tsunamigenic
495 deposits are “characterized by decreased lead concentrations”. Processes associated with this

496 view are described below and illustrated in Figure 8 through a simple conceptual model that
497 can only be applied to older periods.

498 Stage 1: Pre-harbour environment

499 Under coastal pre-harbour conditions (i.e., before the development of port
500 infrastructures associated with the foundation and development of ancient port-cities or
501 activities dealing with lead) no anthropogenic metal excesses are recorded in marine
502 sediments. They can be considered uncontaminated.

503 Stage 2: Functional enclosed harbour environment

504 The development of port-cities and harbour infrastructures thoroughly change the
505 prevailing natural coastline landscape. The decreasing water current velocity induced from the
506 enclosed harbour basin results in lower hydrodynamism that modify in turn the depositional
507 and transport processes of sediments, as well as the geochemical content.. Consequently, finer
508 sediment with higher organic content starts to settle (Fig. 8). During this stage, particle-bound
509 trace metal elements released from urban areas reach the closest urban hydrographic network
510 and, then, reach the harbour basin water column through flows, channels, and canals. In
511 contact with sea water, metallic cations are formed from organo-mineral aggregates
512 (transported on the suspended particulate matter from the river) with the flocculants ions Ca^{2+}
513 and Na^+ from a marine environment. As a result, they massively precipitate at the bottom of
514 the harbour basin. This mixing of fresh and salty waters leads to increase concentrations of
515 trace metal elements into the harbour sediments. In contrast, offshore deposits during ancient
516 periods are uncontaminated due to a significant and fast dilution effect from the
517 uncontaminated open sea water (Fig. 8).

518 Stage 3: Enclosed harbour environment disturbed by a tsunami inundation

519 The tsunami waves trigger the erosion and resuspension of the offshore sediments,
520 which are transported inland and deposited into the harbour basin in the form of an

521 allochthonous coarse layer devoided of anthropogenic metals excesses. The re-suspended
522 sediments from the inner shelf do not contain anthropogenic Pb excesses (“clean” sediments)
523 because it includes sediments deposited prior to the Late Modern Period (post AD 1750)
524 widespread contamination of the seabed (as it is the case during the stage of the pre-harbour
525 environment). At the same time, the landward seawater inundation prevents the river reaching
526 the sea, increasing the intensity of flooding inland, and canceling any chance for heavy metals
527 to be deposited in the harbour basins. Consequently, the allochthonous coarse layers set up by
528 palaeotsunamis in the harbour deposits are characterized by lead concentration levels (also
529 valid for other heavy metals) similar to those of the local environmental Pb background. In all
530 likelihood, the presence of Pb palaeopollutions (anthropogenic Pb excesses) in these coarse
531 deposits definitively dismisses the tsunamigenic hypothesis.

532 Stage 4: Return to a functional harbour environment

533 Once the extreme event is past and stable environmental conditions have been restored,
534 the palaeotsunami deposit is fossilized under a new generation of harbour muds enriched in
535 anthropogenic metal excesses. Stratigraphically, the palaeotsunami deposits trapped into the
536 ancient harbour basins are characterized by a sharp geochemical hiatus.

537

538 *5.2.2. The example of the ancient harbour basin of Ostia*

539 In Figure 3A, Factor 4 indicates the freshwater inflows in the harbour of Ostia
540 (symbolized by negative values) are correlated with metallic pollutants clusters (Pb, Cd, Sn).
541 This specific geochemical fingerprint of the ancient urban waters has been also found in the
542 infilling of the ancient harbour basins of *Portus* (Delile et al., 2014a) testifying its wide
543 coastal extension throughout the Tiber River delta. Their origin has been demonstrated as
544 coming from upstream and related to activities happening in watershed of the Tiber River,
545 including Rome (Delile, 2014 ; Delile et al., 2014b, 2017, 2018). More specifically, Delile et

546 al. (2017) have shown that the direct source of lead contamination trapped in the harbour
547 sediments was solely from the lead pipe system used upstream in the water supply network of
548 Rome and Ostia. Delile et al. (2017) also identified that uncontaminated seawater had diluted
549 contaminated river water. In other words, the Tiber's freshwater transported the upstream
550 originated Pb excesses towards its outlets, including the riverine-coastal harbour basins (Ostia
551 and *Portus*) (Fig. 3B). Downstream uncontaminated marine water inflows diluted the
552 contaminated harbour water columns (Delile et al., 2017, 2018). This process is consistent
553 with the conceptual model described above (Fig. 8). As evidenced by Delile et al. (2017), this
554 marine dilution effect (e.g., Muller and Förstner, 1974) leading to depleted heavy metal
555 concentrations in sediments also concerns “the local coastal environment” of the “Tiber delta
556 deposits” (Hadler et al., 2019), which were likely reworked by smaller high-energy events.
557 For example, in the former Bay of Utica in Tunisia, in which the Medjerda delta was built,
558 based on two deep-sediment cores transects taken towards the ancient offshore environment
559 (Medjerda delta deposits), Delile et al. (2019) observed within 3 km from the outlet,
560 anthropogenic lead (Pb) excesses released into the ancient marine environment are no longer
561 perceptible. Even in the case of a smaller high-energy marine event, a tsunamigenic source of
562 the HEE-3 deposit should be characterized by the lack of Pb excesses in sediments. Clearly,
563 this is not the case (Fig. 3B).

564 Recently, Kolaiti et al. (2017) refuted also the hypotheses of palaeotsunamis deposits
565 proposed by Hadler et al. (2013) based on the high Pb contents recorded in the HEE layers
566 trapped in the sedimentary archives of the Lechaion's ancient harbour basin (ancient Corinth,
567 Greece). Delile et al. (2017) reported that the sedimentary profile of Pb palaeopollution
568 recorded in Unit B2, which is suspected by Hadler et al. (2015) and Wunderlich et al. (2018)
569 to have been deposited by the tsunami HEE-3, “does not fluctuate randomly but displays
570 robust peaks and troughs” (see the curve of the proportion of Pb palaeopollution in Fig. 3B).

571 For all of these reasons, the highly contaminated coarse Unit B2 cannot have been formed by
572 a tsunami event, but instead from increasing fluvial inputs.

573

574 **6. Inconsistencies in the dating of the tsunamis-related HEEs deposits trapped in the**
575 **harbour basin infilling**

576 In this review, we paid particular attention to the radiocarbon and archaeological dates
577 provided by Hadler et al (2015) and Vött et al. (2020). The most important information
578 deduced from radiocarbon dates in palaeotsunami research to strengthen the recognition of
579 tsunamites is the presence of significant chronological inversions inside the high-energy
580 layers (e.g., Nigam and Chaturvedi, 2006 ; Mamo et al., 2009 ; Engel and Brückner, 2011 ;
581 Goiran, 2012; Ishizawa et al., 2020). Strong tsunami deposits are likely to incorporate older
582 organic material dated back to several millennia due to their remobilization induced by
583 erosion of deeper offshore deposits during storm/tsunami events. Figure 7 is a graphical
584 representation of all dates used by Hadler et al. (2015) and Vött et al. (2020) in 2-sigma
585 calibration demonstrating the chronology of the palaeotsunamis history at Ostia. No major
586 inversion can be observed, which does not support the hypothesis of a strong tsunami
587 recorded in the harbour.

588 During the process of this review, we identified inconsistencies in Hadler et al. (2015),
589 between data from their Tables 1 and 2 and the stratigraphies provided in their Figure 7. The
590 dates OST 8/15 PR at -1.74 a.s.l. and OST 8/16 PR at -1.92 a.s.l. comprised between the 10th
591 and 13th c. AD are located in the HEE-3 layer (Fig. 7) reported in Figure 7 from Hadler et al.
592 (2015). However, they are interpreted as a “fluvial deposit” in the interpretative Table 1 from
593 Hadler et al. (2015). Similar errors could also have affected the date OST 2/14 PR 3.34 at -
594 1.49 a.s.l. Despite the absence of a stratigraphic log for the core OST-2 in Hadler et al. (2015),
595 its location halfway between the cores OST-8 (+1.81 m a.s.l.) and OST-3 (+2.29 m a.s.l.)

596 (only 45 meters between these two cores) suggests that the topographic level of the Core
597 OST-2 is ~ +2 m a.s.l. This estimate of the topographic level of the Core OST-2 is confirmed
598 by the difference between the depths of the date OST 2/14 PR expressed in meter a.s.l. (- 1.49
599 meter above present sea level) and m.b.s. (3.34 meter below ground surface), which is + 1.85
600 m a.s.l. Once these precautions are stated, we note that the date OST 2/14 PR (located at a
601 depth of -1.49 m a.s.l.) between the 10th and 13th c. AD is also located into the center part of
602 the HEE-3 layer (Fig. 7) rather than in the assumed upper fluvial deposits (located between
603 +0.25 and -0.5 m a.s.l. into the core OST-8). The mere presence of these too recent dates in
604 the suspected HEE-3 layer suggest that lateral erosion of the Tiber affected the abandoned
605 Roman harbour of Ostia during the Medieval period (Salomon et al., 2016). On the basis of
606 the Figure 7 we can easily read that the real ¹⁴C-based chronological range of the HEE-3
607 facies is ~ 2 millennia (linked to different periods of fluvial activity).

608 Errors are also observed between the photography of Core OST-8 in Figure 3 and its
609 stratigraphy reported in Figure 7 from Hadler et al. (2015). The river harbour and fluvial
610 deposits of Figure 7 should be lower according to the photography of OST-8, and it would
611 replace half of the tsunamigenic deposit hypothesized in Figure 7 from Hadler et al. (2015).
612 Even with this error, the two radiocarbon dates between the 10th and 13th c. AD still date part
613 of the HEE-3 facies in OST-8 (Fig. 7) according to Table 2 in Hadler et al. (2015).

614 Such errors in OST-8 in the stratigraphy and the position of the radiocarbon dates bring
615 confusion to the interpretations. Based on the photography of OST-8 from Figure 3 and Table
616 2 in Hadler et al. (2015), and the review of the palaeoenvironmental data available, we could
617 hypothesise a lateral mobility of the Tiber between 10th and 13th c. AD (possibly part of HEE-
618 3 facies) followed by fine deposition. However, lateral erosion of the Tiber River seems to not
619 have affected cores PO-2 and PO-1 located more south (Goiran et al., 2014).

620 To conclude, we should also point out that the accurate date provided by Vött et al.
621 (2020) of the tsunami-related HEE-7 deposit (“at or shortly after AD 355-363”) is based on an
622 archaeological date (“Mf 21-2”) that were not obtained directly from the Core OST-7A but
623 from an archaeological section (“sondage 21”) located 18 m far from the Core OST-7A. The
624 chronostratigraphic correlation between the Core OST-7A and the archaeological section
625 should be considered carefully especially if we interpret the HEE-7 such as a sandy riverbank
626 deposit (see Fig. 12 in Vött et al., 2020).

627

628 **7. Discussion: flood, storm or tsunami?**

629 Based on palaeoenvironmental data, the previous parts of this paper demonstrate that
630 there is no clear evidence of palaeotsunami deposits at the ancient mouth of the Tiber River.
631 Multi-proxy analyses are the most important evidence to support any interpretation.

632 This section reviews the arguments developed in the discussions proposed by Hadler et
633 al. (2015, 2020) and Vött et al. (2020) about flood, storm or tsunami origin of the HEE layers.
634 We classified elements in their discussion linked to the hypotheses of flood, storm, and
635 tsunami to interpret the high-energy events. We identified four topics of discussion: (1)
636 frequency of events during the Roman period; (2) examples of events during the Roman
637 period; (3) archaeological exposure and possible adjustment; and (4) modern period hazards.
638 The potential factors controlling an eventual tsunami are developed in Hadler et al. (2015,
639 2020) and Vött et al. (2020). Hadler et al. (2015, 2020) refer to the study of Lorito et al.
640 (2008) using tsunami-wave simulations to assign the Southern Tyrrhenian thrust belt, the Tell-
641 Atlas thrust belt, and the western Hellenic arc as the potential source zones of earthquakes
642 triggering long-distance tsunami waves (i.e., teletsunamis). Vött et al. (2020) suggest that the
643 tsunami-induced HEE-7 event was possibly triggered by the AD 365 Crete earthquake. The
644 second cause of tsunamis that authors referred is the volcanic activity in the surrounding area.

645 For instance, based on simulations of volcanic mass failures in the Bay of Naples (Ischia
646 island), the tsunami-induced HEE-1 event could have been triggered by the eruption of the
647 volcanic island of Ischia (Bay of Naples) prior to the 4th c. BC. One of the most famous
648 example of volcano-induced tsunamis in this area concerns the extreme wave event originated
649 from the 79 AD Vesuvius eruption that struck the Roman harbour of Naples (Delile et al.,
650 2016), and was well described in the second letter of Pliny the Younger addressed to Tacitus
651 (Pliny the Younger, VI, 20). Other processes could have triggered tsunami including aerial-
652 subaqueous landslides. However, the Latium holds a low potential for tsunami generation in
653 Italy (Tinti, 1991). As a result, the Latium coastline records a low number of tsunami events
654 yet referenced (Alberico et al., 2018).

655

656 **7.1. Frequency of flood, storm, and tsunami and sedimentary time series**

657 Floods and storms are two very frequent hazards affecting the mouth of the Tiber River
658 (Bellotti et al., 2007, 2018; Goiran et al., 2014; Delile et al., 2018; Salomon et al., 2018;
659 Hadler et al., 2015, 2019). Tsunami events affect the shores of the Latium with much lower
660 frequency (Tinti et al., 2004). One strong argument developed by Hadler et al. (2020)
661 concerns the number of HEE identified. The authors consider that since storm events are very
662 frequent and only 4 to 7 single HEE were observed in the palaeochannel and the harbour of
663 Ostia over the last 3000 years, it implies that tsunamis with low frequency are best-fit
664 statistics for these HEE (Hadler et al., 2020). However, we insist that the sediment traps
665 considered at the mouth of the Tiber cannot provide a good *time series* for storms and
666 tsunamis, and even flood events. During each flood, sediments in active channels are
667 reworked by the river (environment of HEE-4 and 5). Similarly, waves and storms
668 continuously transport sediment along the shore (environment of HEE-1). Regarding the
669 harbour of Ostia, the stratigraphy records only a few centuries and dredging could have

670 affected the regular record of floods and storms (environment HEE-2 and 3) (Salomon et al.,
671 2016; Goiran et al., 2017; Delile et al., 2018). Additionally, the large uncertainty ranges of
672 radiocarbon dates during the second part of 1st millennium BC (Fig. 7) probably do not allow
673 us to identify all dredging activities using hiatuses or inverted dates in the chronology. From
674 such a perspective, the cut-off channel would be better to record a time series of floods and
675 tsunamis (environment of HEE-6). However, in the 16th c. or later, the palaeochannel of Ostia
676 (*Fiume Morto*) would have been too far from the coast to record any storm event.

677 Consequently, we suggest a discussion on HEE frequencies different to Hadler et al.,
678 2020. Considering that the active channel and the shoreface close to the river mouth, there are
679 not reliable sedimentary traps to provide a time series of HEE due to reworking. Additionally,
680 the deposits in the active channel and the shoreface are mainly related to fluvial and coastal
681 processes where single events are difficult to track. In sheltered harbours, single events are
682 easier to identify. However, the quality of the time series of events depends on the recurrence
683 if the dredgings.

684 Roman HEE-3 facies reinterpreted here such as a fluvial deposit occurred during a
685 period known as a major hydro-sedimentary crisis, which increased the frequency of floods in
686 several places of the Western Mediterranean between the 1st c. BC to the 2nd c. AD (Berger
687 and Bravard, 2012), and especially in the Tiber River (Le Gall, 1953; Bersani and
688 Bencivenga, 2001; Salomon, 2013 ; Delile et al., 2014a, 2018; Goiran et al., 2014). HEE-6
689 could express increasing flood frequencies during the Little Ice Age and especially from the
690 end of the 17th c., end of the 18th c. or middle of the 19th c. documented for the Tiber River
691 (Bersani and Bencivenga, 2001; Salomon, 2013).

692

693 **7.2. Events occurring during the Roman period at the mouth of the Tiber River**

694 Single events described by ancient authors are discussed in Hadler et al., 2015,
695 regarding the harbour basins at the mouth of the Tiber River (Ostia and *Portus*). Two ancient
696 texts are quoted, one related to the fluvial harbour of Ostia (Strabo, 5.3.5), the other to the
697 marine Claudian harbour of *Portus* (Tacitus, 15.18.3).

698 One of the most significant quotation is the one of Strabo regarding Ostia, which
699 fortunately matches the place (the harbour of Ostia) and the period (late 1st c. BC / beginning
700 of the 1st c. AD) of the palaeoenvironmental evidence. Several scholars have translated his
701 quote as follows: “[*Ostia*] is harbour less on account of the silting up which is caused by the
702 *Tiber*” (Strabo 5.3.5 after Jones, 1923) or “*Ostia had the inability to maintain or consider a*
703 *convenient sheltered harbour due to the amount of Tiber sediments transported down to the*
704 *seashore*” (Strabo, 5.3.5 after P. Arnaud, in Goiran et al., 2014) or “*This city has no port,*
705 *owing to the accumulation of the alluvial deposit brought down by the Tiber, which is swelled*
706 *by numerous rivers*” (Strabo, 5.3.5 after Hamilton and Falconer, 1903). In our opinion, the
707 reference to this text corroborates the quick sedimentation of silts in the harbour (Goiran et
708 al., 2014; Hadler et al., 2015), but especially to the deposition of the fluvial bedload-derived
709 deposit on top (HEE-3 - Figs. 2 and 3) (Goiran et al., 2014; Delile et al., 2018).

710 Although the quotation of Strabo (5.3.5) is more appropriate in discussing the
711 interpretation of the sedimentary drilling of the harbour of Ostia, the storm described by
712 Tacitus is widely discussed by Hadler et al., 2015 (“*some two hundred vessels [...] had been*
713 *destroyed by a raging tempest*” in 62 AD - Tacitus, 15.18.3 after Jackson, 1937). This
714 quotation does not match in space (Claudian harbour) and time (after the abandonment of the
715 Ostia harbour) any of the HEEs identified in the harbour of Ostia. Additionally, the possibility
716 of this AD 62 event was a tsunami is for now, only hypothetical. Finally, no evidence of the
717 AD 62 deposit was found on top of HEE-3 in the area of the harbour of Ostia (OST-3) or in
718 any other core.

719

720 **7.3. Risk exposure in the Tiber River delta during the Roman period**

721 Arguments based on archaeological data are used in Hadler et al. (2015 and 2020) to
722 discredit hypotheses of floods and storms for the HEE-2 and 3. For the authors, the presence
723 of warehouses called *horrea* along the Tiber River in Ostia suggests that, “Tiber floods were
724 seen as well-manageable natural events rather than as an unscalable hazard” (Hadler et al.,
725 2015 and similar argument in 2020). Floods of the Tiber were a major concern during the
726 Roman period and many solutions were considered or applied to reduce this risk (Le Gall,
727 1953; Aldrete, 2007; Cappelletti, 2009). However, there is no such thing as zero risk in the
728 past, as well as the present time. Even though engineered solutions were probably developed
729 during the Roman period to reduce flood and fluvial depositions in the harbour of Ostia,
730 floods could still have been deposited, and fluvial inundation could have affected the
731 structures. Consequences of floods could have been “seen as well-manageable natural events”
732 by Romans (Hadler et al., 2015), but it did not prevent all kind of HEE to happen. Accelerated
733 siltation of numerous harbour basins are observed along the shores of the Mediterranean Sea,
734 such as that of the Roman harbour of Narbonne in the 1st c. (Rescanières, 2002), and those of
735 Frejus (Excoffon et al., 2010), Ephesus (Stock et al., 2016 ; Delile et al., 2015), Naples (Delile
736 et al., 2016), Pisa (Benvenuti et al., 2006; Mariotti Lippi et al., 2007), as well as that *Portus*
737 (Pepe et al., 2013; Delile et al., 2014a).

738 Similarly, the presence of Roman villas along the coast at the south of Ostia is supposed
739 to attest to “a generally minor vulnerability of the Latium coastal area to storms” in Hadler et
740 al., (2015 and similar argument in 2020). It should be noticed many research conducted about
741 risks, its perceptions, and the level of acceptance of risks by populations (Arnaud-Fassetta et
742 al., 2010; Bradford et al., 2012). It should be more a research question than a statement.

743

744 **7.4. Modern evidence on extreme floods, storms and tsunamis that affected the Lower**
745 **Tiber floodplain and the Latium coast**

746 While modern occurrences and frequencies of extreme storms and tsunamis are largely
747 discussed in Hadler et al. (2015, 2020), less is developed about extreme floods. We interpret
748 HEE-3, 7, 4, 5 and 6 as mainly driven by fluvial processes, and are willing to also
749 demonstrate the strength of extreme Tiber River floods. However, we are not denying the
750 violence of extreme storms (Noli et al., 1996; Cavichia et al., 2014) and tsunamis (Tinti et al.,
751 2004) that could affect the coasts of the Latium.

752 Among the floods of the Tiber River, summer floods can be extremely powerful and
753 transport large amounts of sediments – e.g. in 1530, 1557, 1868 and 1965 (Bersani et al.,
754 2004). During the summer flood of 1557, the palaeomeander of Ostia was cut-off and the
755 *Ponte Rotto* in Rome was damaged. More recently in 1965, a summer flood led to the collapse
756 of bridges in the Tiber River watershed, and flooded a large area of Maccarese (Bersani et al.,
757 2004). However, the majority of Tiber River floods occurs in winter. Tiber River winter
758 floods can be exceptional and particularly damaging, carrying large amounts of sediment. The
759 strongest historical flood ever recorded occurred the 24th of September 1598 reaching 19.56 m
760 at Ripetta, and was particularly damaging to Rome (Bersani and Bencivenga, 2001). Flood
761 series based on historical records are available for Rome in Le Gall (1953) and Bersani &
762 Bencivenga (2001).

763

764 **7.5. Big storm or small tsunami?**

765 Hadler et al. (2015, 2020) promote a sea-born origin of most of the HEE identified in
766 Ostia that raises the issue of the identification of the marine-born processes triggering these
767 HEEs, i.e., storm and tsunamis. Hadler et al. (2020) also develop the hypothesis of minor
768 tsunamis inundating the coastal area: “Although ancient Ostia is not prone to exceptionally

769 strong tsunami events, the mouth of the Tiber River could provide a potential pathway where
770 even minor tsunami inundation would be capable of leaving a signal in the sedimentary
771 record” (Hadler et al., 2020). It results in even more difficulties to identify clear evidence
772 between small tsunamis and strong storms.

773 We are not denying these minor tsunamis occur along the coast of the Latium. In fact,
774 modern texts describe some of these small events (Tinti et al., 2004). However, because major
775 tsunami deposits are already difficult to identify in river mouth environments, evidence of
776 minor tsunami deposits should be even harder to track. The river mouth of the Tiber is
777 definitely not the right area to look for palaeoenvironmental evidence of these kinds of natural
778 hazards.

779 One of the main arguments in excluding a storm origin of the coarsest deposits recorded
780 in the Ostia’s harbour basin is that storm waves could not reach the site of the harbour basin,
781 because today no storm would be able “to inundate far beyond the present coastline” (Hadler
782 et al., 2015) (Fig. 1). We must recall that the coastline was located around 150 m and 500 m
783 away from the ancient harbour basin during the 4th c. BC and the 2nd / 3rd c. AD, respectively
784 (Goiran et al., 2014, Salomon et al., 2018) (Fig. 1). On the other hand, in their database
785 compiling criteria for distinguishing tsunami from storm deposits, Morton et al. (2007) report
786 that storm deposits are restricted to a few hundred meters zone from the shore. For their part,
787 Morton and Sallenger (2003) note that only the most powerful storms, i.e. those contained
788 into the third quartile (25% of the most powerful storms), can transport sand more than 300 m
789 inland, depending on the morphology of the coastline. As a result, these statements argue that
790 storm deposits have easily reached the harbour basin of Ostia during ancient times given the
791 distance separating it from the coastline at these periods. In this regard, the storm hypotheses
792 should still be considered.

793 Additionally, based on the study of the Mediterranean's Medicanes (from
794 *Mediterranean hurricanes*, i.e. tropical-like Mediterranean storm) done by Cavicchia et al.
795 (2014), Hadler et al. (2015) consider it unlikely that the coastal area of Latium experienced
796 "major storm surges" in the past. Actually, one medicane was registered in the last 60 years
797 off the coast of the Latium. This study also demonstrates that medicanes form preferentially in
798 the Western Mediterranean, and the percentage of days on which favorable environmental
799 conditions are found along the Latium coast is comprised of between 0.3 and 0.4. It does not
800 exceed 1% because medicanes are rare storms (Cavicchia et al., 2014). Moreover, no details
801 are provided in this study on the distribution of land falling sites of medicanes, while once
802 formed they can travel hundreds of kilometers offshore before land falling. Finally, this
803 meteo-marine phenomenon of medicanes is only one of the type of storms that may occur in
804 the Mediterranean basin among other more common types (Lionello et al., 2016).

805 **8. Conclusions**

806 This study has aimed to review all of the proxies currently documenting the sedimentary
807 archives of different environments at the mouth of the Tiber River to test the recent
808 hypothesis made by Hadler et al. (2015, 2020), Wunderlich et al. (2018) and Vött et al. (2020)
809 of the occurrence of several tsunamis, which struck Ostia between the 8^e c. BC and the 17th c.
810 AD or later. Based on all of the indicators available (sedimentological, geomorphological,
811 geochemical, chronological, microfaunistic, archaeological and historical data), we consider
812 that there is no clear evidence of tsunami inundations at the mouth of the Tiber River
813 (shoreface / river mouth, harbour or the palaeochannel of Ostia). Fluvio-coastal environments
814 are complex environments where finding clear evidence of palaeotsunami deposits is
815 challenging (Mamo et al., 2009 ; Engel and Brückner, 2011 ; Chagué-Goff et al. 2017 ;
816 Marriner et al., 2017 ; Röbbke and Vött, 2017) (Fig. 9).

817 In our opinion, the formation of HEE-1 is formed from a specific geomorphological
818 feature (river mouth bar-through) and mixed fluvio-coastal processes where no single
819 flood/storm/tsunami can be identified. Several research groups identified this layer in coastal
820 areas near the palaeoriver mouth of the Tiber River (Giraudi et al., 2009; Salomon, 2013;
821 Milli et al., 2013; Goiran et al., 2014; Delile et al., 2018).

822 HEE-2 is trapped in the harbour of Ostia. It is a single event but no evidence allows us
823 to determine its origin (flood/storm/tsunami). This interpretation is based only on a
824 reinterpretation of the data from Hadler et al. (2015). However, it is surprising that among the
825 ten cores taken in the ancient harbour basin of Ostia (about 2.5 ha) (Fig. 1), only Cores OST-3
826 and PO-1 recorded the HEE-2 layer. Additionally, the existence of estuarine assemblages of
827 autochthonous foraminifers developing in the lower reach of the Tiber River should be
828 considered. It would probably contribute to better understand the complexity of the river
829 mouth environments and improve the interpretation of all the cores reviewed here.

830 HEE-3 sealed the harbour of Ostia. It is definitely from fluvial origin based on
831 palaeoenvironmental data from Hadler et al. (2015), Goiran et al. (2014), Sadori et al. (2016),
832 Vött et al. (2020), and geochemical data from Delile et al. (2017, 2018). The processes
833 involved and leading to the presence of foraminifers in flood deposits should be explored
834 (e.g., floating foraminifers, autochthonous foraminifers developing between flood events).

835 HEE-7 would be most likely a semi-protected sandy riverbank developing in a chamber
836 of the shipshed of Ostia. This layer was deposited at the level of the ancient sea level (Goiran
837 et al., 2009; Heinzelmann et al., 2020). In this context, the high quantity of foraminifers
838 identified by Vött et al., 2020, could be related to their floating and/or swashing on the
839 riverbank. Clearly, this hypothesis should be confirmed by studying current sandy riverbank
840 near the mouth of the Tiber River.

841 HEE-4 and 5 are located in the ancient active channel of the Tiber River. In this context,
842 fluvial high-energy events are reworked by other fluvial high-energy events. Most of the
843 sedimentation is controlled by fluvial dynamics, but affected seasonally by salt wedge
844 intrusions. It results in a complex stratigraphy where identifying specific events of floods or
845 any other natural hazards (storm/tsunami) is almost impossible. In our opinion, none of the
846 sedimentological, or palaeoenvironmental data for now available from Hadler et al. (2020) or
847 Salomon et al. (2017) can provide clear evidence of palaeotsunami deposits.

848 Finally, HEE-6 located in the floodplain and at the last infill stage of the palaeomeander
849 of Ostia demonstrates an event bracketed within a slow increase and decrease of the grain size
850 with all similar estuarine assemblage of foraminifers. We would interpret this change in Unit
851 D in Core TEV-1A as flood deposits settled during a period of major inundations of the Tiber
852 River during the last centuries of the Little Ice Age. More data would be required to support
853 the tsunami hypothesis.

854 We acknowledge that the tsunami hypothesis should be considered more often among
855 other more common processes when interpreting palaeoenvironmental data, especially in the
856 Mediterranean. However, when looking for tsunamis, the depositional context is crucial
857 (Shanmugam, 2012). Palaeotsunamis may have affected the mouth of the Tiber, but
858 geomorphological and palaeoenvironmental evidence should be identified in other areas along
859 the coast of the Latium. Lagoons and harbour basins far from river mouth environments
860 would provide more reliable data. Additionally, the identification of geomorphological and
861 palaeoenvironmental evidence of tsunamis from the same period separated by several
862 kilometers would reinforce the tsunami hypothesis.

863

864 Even if each pluridisciplinary evidence has to be considered as a complementary source
865 of information to identify palaeotsunami deposits, we believe that some of them are
866 particularly useful, and therefore, require special attention in this type of study.

867 (i) The *chronology* of palaeotsunami events trapped in sedimentary archives should be
868 supported by dates directly obtained from the high-energy deposits, or at least as close as
869 possible to them. Moreover, it is imperative that all of the dates conducted are readable
870 directly on the stratigraphic logs.

871 (ii) Some *geomorphological features* may be relevant to the identification of processes
872 involved in high-energy deposits. First, the spatial continuity of the tsunami layers in the
873 harbour basins should be observed. In practical terms, this means that tsunamites should be
874 identified in a large majority of cores taken in the area, which is presumed to have
875 experienced past tsunami events. The distinction between a storm and a tsunamigenic origin
876 requires, among other factors/variables, knowing the evolution of the palaeoshoreline
877 positions over time, including the coastal evolution in palaeotsunamis research (Garrett et al.,
878 2016).

879 (iii) *Micropalaeontology*, and more specifically *foraminiferal assemblages*, are known to
880 be powerful tools in identifying high-energy marine events. The best foraminiferal evidence
881 for tsunami sediments contain deep water assemblages and/or, to a lesser extent, sudden
882 displaced assemblages, and a higher species diversity (Dawson et al., 1995; Hindson and
883 Andrade, 1999; Hindson et al., 1996, 1998; Hawkes et al., 2007; Mamo et al., 2009).

884 (iv) *Elemental geochemistry* has also become an essential tool to the study of
885 palaeotsunamis because it can identify both sedimentary sources and the fluvial or marine
886 transport vector (Chagué-Goff et al., 2017). At Ostia, this approach has shown a gradual and
887 continuous regression of seawater influence within Core PO-2 stratigraphy due to the
888 freshwater inputs (Delile et al., 2018).

889 (v) *Heavy metal palaeopollutions* might easily help to identify palaeotsunamites based
890 on their presence or absence. The palaeotsunami sediments anterior to the Late Modern
891 Period (post AD 1750) are known to be devoid of any traces of Pb palaeopollutions (Hadler et
892 al., 2013; Finkler et al., 2018a,b; Kolaiti et al., 2017). At Ostia, the presence of anthropogenic
893 Pb excesses fluctuating over times consistently with robust peaks and troughs in the coarsest
894 sediments (Delile et al., 2017) invalidate the youngest tsunami event.

895 If clear evidence suggests palaeotsunami events in Ostia or on the coast of Lazio, this
896 would be of major importance. However, based on the dataset reviewed, none of the HEE
897 layers identified around Ostia suggest a clear palaeotsunami origin. Even if we consider the
898 importance of the geomorphological and sedimentological impacts of high-energy events, we
899 would like to point out the extreme geomorphological variability of coastal environments, in
900 particular river mouth environments. Such a highly mobile deposit environment appears to be
901 not suitable in the reconnaissance of palaeotsunamis deposits, and therefore requires all the
902 more caution for multi-proxy interpretations. We still consider the palaeotsunami hypothesis
903 seriously, and it should be examined carefully in balance with other fluvial and coastal
904 processes.

905

906 **Acknowledgments**

907 We thank the *Soprintendenza Speciale per i Beni Archeologici di Roma - Sede di Ostia*
908 for the permission to drill core PO-2 in the ancient harbour basin of Ostia. We further
909 acknowledge the ARTEMIS-SHS program and radiocarbon laboratory of Lyon for
910 conducting the radiocarbon dating. The Young Scientist Program of the Agence Nationale de
911 la Recherche (CNRS) (ANR 2011 JSH3 002 01), the Roman Mediterranean Ports program
912 (ERC grant agreement n° 339123), and the Ecole Française de Rome provided financial and
913 logistic support. Finally, we are grateful to Jean-Philippe Goiran, Cécile Vittori for our useful

914 discussions on this issue of palaeotsunami deposits at the Tiber River mouth and their
915 insightful advices. Finally, we would like to thanks the two anonymous reviewers for their
916 valuable remarks and comments, which significantly contributed to the quality of the paper.

917

918 **References**

919 Alberico, I., Budillon, F., Casalbore, D., Di Fiore, V., Iavarone, R., 2018. A critical review of
920 potential tsunamigenic sources as first step towards the tsunami hazard assessment for
921 the Napoli Gulf (Southern Italy) highly populated area. *Nat Hazards* 92, 43–76.

922

923 Aldrete, GS, (2007) *Floods of the Tiber in ancient Rome*. Baltimore: The Johns Hopkins
924 University Press.

925 Arnaud-Fassetta, G, Carcaud, N, Castanet, C et al. (2010). Fluvial palaeoenvironments in
926 archaeological context: Geographical position, methodological approach and global
927 change – Hydrological risk issues. *Quaternary International* 216: 93-117.

928 Bellotti, P, Calderoni G, Carboni MG, et al. (2007) Late Quaternary landscape evolution of
929 the Tiber River delta plain (Central Italy): new evidence from pollen data,
930 biostratigraphy and 14C dating. *Zeitschrift für Geomorphologie* 51(4): 505–534.

931 Bellotti, P., Calderoni, G., Rita, F.D., D'Orefice, M., D'Amico, C., Esu, D., Magri, D.,
932 Martinez, M.P., Tortora, P., Valeri, P., 2011. The Tiber river delta plain (central Italy):
933 coastal evolution and implications for the ancient Ostia Roman settlement. *Holocene*
934 21, 1105-1116.

935 Bellotti, P., Davoli, L., Sadori, L. (2018) Landscape diachronic reconstruction in the Tiber
936 delta during historical time: a holistic approach. *Geografia Fisica e Dinamica*
937 *Quaternaria* 41: 3-21.

938 Benvenuti M, Mariotti-Lippi M, Pallecchi P, et al. (2006) Late-Holocene catastrophic floods
939 in the terminal Arno River (Pisa, Central Italy) from the story of a Roman riverine
940 harbour. *The Holocene* 16(6): 863–876.

941 Bersani, P. and Bencivenga, M. *Le Piene del Tevere a Roma dal V secolo a.C. all'anno 2000*
942 (2001). Servizio Idrografico e Mareografico Nazionale. Rome: Presidenza del
943 Consiglio dei Ministri Dipartimento per i Servizi Tecnici Nazionali.

944 Berger J-F and Bravard J-P (2012) Le développement économique romain face à la crise
945 environnementale : le cas de la Gaule narbonnaise. In: *Des Climats et Des Hommes*.
946 La Découverte. Paris: Berger, J.-F., pp. 269–289.

947 Bersani P and Bencivenga M (2001) *Le piene del Tevere a Roma dal V secolo a.C. all'ano*
948 *2000*. Servizio idrografico e mareografico nazionale. Roma: Dipartimento per i Servizi
949 Tecnici Nazionali.

950 Bersani, P (2004) Tiber River at Rome: summer floods and considerations on the maximum

- 951 historical discharge. *Geologia Tecnica e Ambientale* 2: 23-68.
- 952 Bradford, RA, O'Sullivan, JJ, Van der Craats, IM (2012) Risk perception–issues for flood
953 management in Europe. *Natural Hazards and Earth System Science* 12: 2299–2309.
- 954 Capelli, G. and Mazza, R. (2008). « Intrusione salina nel delta del fiume Tevere. Evoluzione
955 del fenomeno nei primi anni del terzo millennio ». In *La geologia di Roma: dal Centro
956 Storico alla Periferia - Seconda Parte*, 80:237-60. Memorie descrittive della Carta
957 Geologica d'Italia. Firenze: S.EL.C.A..
- 958 Cappelletti S. 2009, Il progetto sull'esonazione del Tevere, *ACME* LXII, 235-253.
- 959 Cavicchia L, Storch H von and Gualdi S (2014) A long-term climatology of medicanes.
960 *Climate Dynamics* 43(5–6): 1183–1195.
- 961 Chagué-Goff C, Szczuciński W and Shinozaki T (2017) Applications of geochemistry in
962 tsunami research: A review. *Earth-Science Reviews* 165: 203–244.
- 963 Dawson AG, Long D and Smith DE (1988) The Storegga Slides: Evidence from eastern
964 Scotland for a possible tsunami. *Marine Geology* 82(3): 271–276.
- 965 Dawson AG, Hindson R, Andrade C, et al. (1995) Tsunami sedimentation associated with the
966 Lisbon earthquake of 1 November AD 1755: Boca do Rio, Algarve, Portugal. *The
967 Holocene* 5(2): 209–215.
- 968 Delile H (2014) *Signatures des paléo-pollutions et des paléoenvironnements dans les archives
969 sédimentaires des ports antiques de Rome et d'Éphèse*. Doctorat de géographie /
970 géoarchéologie. Université Lumière Lyon 2, Lyon.
- 971 Delile H, Mazzini I, Blichert-Toft J, et al. (2014a) Geochemical investigation of a sediment
972 core from the Trajan basin at Portus, the harbor of ancient Rome. *Quaternary Science
973 Reviews* 87: 34–45.
- 974 Delile H, Blichert-Toft J, Goiran J-P, et al. (2014b) Lead in ancient Rome's city waters.
975 *Proceedings of the National Academy of Sciences* 111(18): 6594–6599.
- 976 Delile H, Blichert-Toft J, Goiran J-P, et al. (2015) Demise of a harbor: A geochemical
977 chronicle from Ephesus. *Journal of Archaeological Science* 53: 202–213.
- 978 Delile H, Goiran J-P, Blichert-Toft J, et al. (2016) A geochemical and sedimentological
979 perspective of the life cycle of Neapolis harbor (Naples, southern Italy). *Quaternary
980 Science Reviews* 150: 84–97.
- 981 Delile H, Keenan-Jones D, Blichert-Toft J, et al. (2017) Rome's urban history inferred from
982 Pb-contaminated waters trapped in its ancient harbor basins. *Proceedings of the
983 National Academy of Sciences* 114(38): 10059–10064.
- 984 Delile H, Goiran JP and Blichert-Toft J (2018) The contribution of geochemistry to ancient
985 harbor geoarcheology: The example of Ostia Antica. *Quaternary Science Reviews*
986 193: 170–187.
- 987 Delile, H, Pleuger, E, Blichert-Toft, J et al. (2019). Economic resilience of Carthage during

- 988 the Punic Wars: Insights from sediments of the Medjerda delta around Utica (Tunisia).
989 *Proceedings of the National Academy of Sciences* 116: 9764–9769.
990
- 991 Di Bella, L., Bellotti, P., Frezza, V., Bergamin, L., Carboni, M.G. (2011). « Benthic
992 Foraminiferal Assemblages of the Imperial Harbor of Claudius (Rome): Further
993 Paleoenvironmental and Geoarcheological Evidences ». *The Holocene* 21, n° 8:
994 1245-59.
- 995 Di Bella, L., Bellotti, P., Milli, S. (2013). « The Role of Foraminifera as Indicators of the
996 Late Pleistocene–Holocene Palaeoclimatic Fluctuations on the Deltaic Environment:
997 The Example of Tiber Delta Succession (Tyrrhenian Margin, Italy) ». *Quaternary
998 International* 303: 191-209.
- 999 Engel M and Brückner H (2011) The identification of palaeo-tsunami deposits – a major
1000 challenge in coastal sedimentary research. In: *Dynamische Küsten – Prozesse,
1001 Zusammenhänge Und Auswirkungen*. Coastline Reports 17. Karius, Hadler, Deicke,
1002 von Eynatten, Brückner & Vött, pp. 65–80.
- 1003 Excoffon P, Bonnet S, Devillers B et al. (2010) L'évolution du trait de côte aux abords de
1004 Fréjus de sa fondation jusqu'à la fin du 1er s. ap. J.-C. In: *Archéologie Des Rivages
1005 Méditerranéens : 50 Ans de Recherche*. Errance. Delestre, X., pp. 47–53.
- 1006 Finkler C, Fischer P, Baika K, et al. (2018a) Tracing the Alkinoos Harbor of ancient Kerkyra,
1007 Greece, and reconstructing its paleotsunami history. *Geoarchaeology* 33(1): 24–42.
- 1008 Finkler C, Baika K, Rigakou D, et al. (2018b) Geoarchaeological investigations of a
1009 prominent quay wall in ancient Corcyra – Implications for harbour development,
1010 palaeoenvironmental changes and tectonic geomorphology of Corfu Island (Ionian
1011 Islands, Greece). *Quaternary International* 473. Integrated geophysical and
1012 (geo)archaeological explorations in wetlands: 91–111.
- 1013 Garrett, E, Fujiwara, O, Garrett, P et al. (2016) A systematic review of geological evidence
1014 for Holocene earthquakes and tsunamis along the Nankai-Suruga Trough, Japan.
1015 *Earth-Science Reviews* 159: 337–357.
1016
- 1017 Goff J, Chagué-Goff C and Nichol S (2001) Palaeotsunami deposits: a New Zealand
1018 perspective. *Sedimentary Geology* 143: 1–6.
- 1019 Giraudi, C, Tata, C, Paroli, L (2009). Late Holocene evolution of Tiber river delta and
1020 geoarchaeology of Claudius and Trajan Harbor, Rome. *Geoarchaeology* 24: 371-82.
- 1021 Goiran J-P, Salomon F, Pleuger E, et al. (2012) Port antique d'Ostie. *Chronique des activités
1022 archéologiques de l'École française de Rome* 123(2): 1–7.
- 1023 Goiran J-P, Salomon F, Mazzini I, et al. (2014) Geoarchaeology confirms location of the
1024 ancient harbour basin of Ostia (Italy). *Journal of Archaeological Science* 41: 389–398.
- 1025 Goiran J-P, Salomon F, Vittori C, et al. (2017) High chrono-stratigraphal resolution of the
1026 harbour sequence of Ostia: palaeo-depth of the bassin, ship drought & dredging. In:
1027 *Fluvial Landscapes in the Roman World: Rivers and their influences on Roman life,*
1028 Portsmouth, 2017, pp. 67–83. *Journal of Roman Archaeology: Supplementary Series.*
1029 T. Franconi.

- 1030 Hadler H, Vött A, Koster B, et al. (2013) Multiple late-Holocene tsunami landfall i in the
1031 eastern Gulf of Corinth recorded in the palaeotsunami geo-archive at Lechaion,
1032 harbour of ancient Corinth (Peloponnese, Greece). *Zeitschrift für Geomorphologie*
1033 57(4): 139–180.
- 1034 Hadler H, Vött A, Fischer P, et al. (2015) Temple-complex post-dates tsunami deposits found
1035 in the ancient harbour basin of Ostia (Rome, Italy). *Journal of Archaeological Science*
1036 61: 78–89.
- 1037 Hadler H, Fischer P, Obrocki L, et al. (2020) River channel evolution and tsunami impacts
1038 recorded in local sedimentary archives – the ‘Fiume Morto’ at Ostia Antica (Tiber
1039 River, Italy). *Sedimentology* 67: 1309–1343.
- 1040 Hamilton, H. C. and Falconer, W. (1903). The Geography of Strabo. Literally translated, with
1041 notes, in three volumes. London. George Bell & Sons.. ed. H.C. Hamilton, Esq., W.
1042 Falconer, M.A.
- 1043 Hawkes AD, Bird M, Cowie S, et al. (2007) Sediments deposited by the 2004 Indian Ocean
1044 Tsunami along the Malaysia–Thailand Peninsula. *Marine Geology* 242(1): 169–190.
- 1045 Heinzelmann M and Martin A (2002) River port, navalia, and harbour temple at Ostia: new
1046 results of a DAI-AAR Project. *Journal of Roman Archaeology* 15: 5–29.
- 1047 Heinzelmann M (2020) Forma Urbis Ostia 1. Ergebnisse der stratigraphischen
1048 Untersuchungen in den unausgegrabenen Stadtgebieten. Reichert-Verlag, Wiesbaden
1049 (in press)
- 1050 Hindson RA and Andrade C (1999) Sedimentation and hydrodynamic processes associated
1051 with the tsunami generated by the 1755 Lisbon earthquake. *Quaternary International*
1052 56(1): 27–38.
- 1053 Hindson RA, Andrade C and Dawson AG (1996) Sedimentary processes associated with the
1054 tsunami generated by the 1755 Lisbon earthquake on the Algarve coast, Portugal.
1055 *Physics and Chemistry of the Earth* 21(1). Tsunamis Impacting on the European
1056 Coasts: Modelling, Observation and Warning: 57–63.
- 1057 Hindson R, Andrade C and Parish R (1998) A microfaunal and sedimentary record of
1058 environmental change within the late Holocene sediments of Boca do Rio (Algarve,
1059 Portugal). *Geologie en Mijnbouw* 77(3–4): 311–321.
- 1060 Ishizawaa T, Goto, K, Yokoyama, Y, Goff, J (2020) Dating tsunami deposits: Present
1061 knowledge and challenges. *Earth-Science Reviews* 200: 102971.
- 1062 Jackson, J., 1937. Tacitus. Annals. Books 13-15. Harvard University Press, Cambridge/
1063 London.
- 1064 Jones, H.L. (1923). Geography of Strabo. In: Books 3-5, vol. II. Harvard University Press,
1065 Cambridge/London
- 1066 Kolaiti E, Papadopoulos GA, Morhange C, et al. (2017) Palaeoenvironmental evolution of the
1067 ancient harbor of Lechaion (Corinth Gulf, Greece): Were changes driven by human
1068 impacts and gradual coastal processes or catastrophic tsunamis? *Marine Geology* 392:

- 1069 105–121.
- 1070 Le Gall J (1953) *Le Tibre, Fleuve de Rome Dans l'Antiquité*. Paris: Presses universitaires de
1071 France.
- 1072 Lionello, P, Trigo, IF, Gil, V, Liberato, MLR et al. (2016) Objective climatology of cyclones
1073 in the Mediterranean region: a consensus view among methods with different system
1074 identification and tracking criteria. *Tellus A: Dynamic Meteorology and*
1075 *Oceanography* 68: 29391.
- 1076 Lorito, S., Tiberti, M.M., Basili, R., Piatanesi, A., Valensise, G., 2008. Earthquake-generated
1077 tsunamis in the Mediterranean Sea: Scenarios of potential threats to Southern Italy.
1078 *Journal of Geophysical Research: Solid Earth* 113.
1079
- 1080 Maramai A., Brizuela B., Graziani L. (2014) The Euro-Mediterranean Tsunami Catalogue,
1081 *Annals of Geophysics*, 57: 4,
- 1082 Manca, F., Capelli, G., La Vigna, F., Mazza, R., Pascarella, A. (2014) « Wind-Induced Salt-
1083 Wedge Intrusion in the Tiber River Mouth (Rome–Central Italy) ». *Environmental*
1084 *Earth Sciences* 72, n° 4: 1083-95.
- 1085 Mamo B, Strotz L and Dominey-Howes D (2009) Tsunami sediments and their foraminiferal
1086 assemblages. *Earth-Science Reviews* 96(4): 263–278.
- 1087 Mariotti Lippi M, Bellini C, Trinci C, et al. (2007) Pollen analysis of the ship site of Pisa San
1088 Rossore, Tuscany, Italy: the implications for catastrophic hydrological events and
1089 climatic change during the late Holocene. *Vegetation History and Archaeobotany*
1090 16(6): 453–465.
- 1091 Marriner N, Kaniewski D, Morhange C, et al. (2017) Tsunamis in the geological record:
1092 Making waves with a cautionary tale from the Mediterranean. *Science Advances*
1093 3(10): 12.
- 1094 Mazzini I, Faranda C, Giardini M, et al. (2011) Late Holocene palaeoenvironmental evolution
1095 of the Roman harbour of Portus, Italy. *Journal of Paleolimnology* 46(2): 243–256.
- 1096 Mikhailova, M. V., Bellotti, P., Tortora, P., Valeri, P. (1999) « Intrusion of seawater into the
1097 river part of the Tiber mouth ». *Water Resources* 26.
- 1098 Milli S, D'Ambrogi C, Bellotti P, et al. (2013) The transition from wave-dominated estuary to
1099 wave-dominated delta: The Late Quaternary stratigraphic architecture of Tiber River
1100 deltaic succession (Italy). *Sedimentary Geology* 284: 159–180.
- 1101 Morton RA and Sallenger AH (2003) Morphological Impacts of Extreme Storms on Sandy
1102 Beaches and Barriers. *Journal of Coastal Research* 19(3): 560–573.
- 1103 Morton RA, Gelfenbaum G and Jaffe BE (2007) Physical criteria for distinguishing sandy
1104 tsunami and storm deposits using modern examples. *Sedimentary Geology* 200(3).
1105 Sedimentary Features of Tsunami Deposits - Their Origin, Recognition and
1106 Discrimination: An Introduction: 184–207.
- 1107 Müller, G and Förstner, U (1975). Heavy metals in sediments of the rhine and elbe estuaries:

- 1108 Mobilization or mixing effect? *Environmental Geology* 1 (1) 33–39.
- 1109 Nigam R and Chaturvedi SK (2006) Do inverted depositional sequences and allochthonous
1110 foraminifers in sediments along the Coast of Kachchh, NW India, indicate
1111 palaeostorm and/or tsunami effects? *Geo-Marine Letters* 26(1): 42–50.
- 1112 Noli, P., De Girolamo, P., Sammarco, P., « Parametri meteomarini e dinamica costiera ». Il
1113 mare del Lazio. Università “La Sapienza” di Roma, Regione Lazio Assessorato opere
1114 e reti di servizi e mobilità, 1996.
- 1115 Paris R, Lavigne F, Wassmer P et al. (2007) Coastal sedimentation associated with the
1116 December 26, 2004 tsunami in Lhok Nga, west Banda Aceh (Sumatra, Indonesia).
1117 *Marine Geology* 238(1): 93–106.
- 1118 Pepe, C., Giardini, M., Giraudi, C. et al. (2013). Plant landscape and environmental changes
1119 recorded in marginal marine environments: The ancient Roman harbour of Portus
1120 (Rome, Italy). *Quaternary International* 303: 73–81.
1121
- 1122 Pepe, C, Sadori, L, Andrieu-Ponel, V et al. (2016) Late Holocene pollen record from Fiume
1123 Morto (Dead River), a palaeomeander of Tiber River near Ancient Ostia (central
1124 Italy). *Journal of Paleolimnology* 56: 173–187.
1125
- 1126 Pignatelli, C., Sansò, P., Mastronuzzi, G., 2009. Evaluation of tsunami flooding using
1127 geomorphologic evidence. *Marine Geology* 260, 6–18.
1128
- 1129 Pliny the Younger, Quintilien, 1858. Oeuvres complètes, Collection des auteurs
1130 latins. Firmin Didot, Paris, France.
1131
- 1132 Rescanières S (2002) Essai sur le cadre géographique antique du Narbonnais. In: *Narbonne et*
1133 *Le Narbonnais*. Carte archéologique de la Gaule 11/1. Paris: Dellong, E., pp. 44–51.
- 1134 Röbbke BR and Vött A (2017) The tsunami phenomenon. *Progress in Oceanography* 159:
1135 296–322.
- 1136 Rubin CM, Horton BP, Sieh K, et al. (2017) Highly variable recurrence of tsunamis in the
1137 7,400 years before the 2004 Indian Ocean tsunami. *Nature Communications* 8: 16019.
- 1138 Ruiz, F., González-Regalado, M. L., Pendón, J. G., Abad, M., Olías, M., Muñoz, J. M. (2005).
1139 « Correlation between foraminifera and sedimentary environments in recent estuaries
1140 of Southwestern Spain: Applications to holocene reconstructions ». *Quaternary*
1141 *International*, 140–141: 21–36.
- 1142 Sadori L, Mazzini I, Pepe C, et al. (2016) Palynology and ostracodology at the Roman port of
1143 ancient Ostia (Rome, Italy). *The Holocene* 26(9): 1502–1512.
- 1144 Salomon F (2013) *Géoarchéologie du delta du Tibre*. PhD thesis. Lumière Lyon 2.
- 1145 Salomon P, Delile H, Goiran J-P, et al. (2012) The Canale di Comunicazione Traverso in
1146 Portus: the Roman sea harbour under river influence (Tiber delta, Italy).
1147 *Géomorphologie : relief, processus, environnement*, (1): 75–90.
- 1148 Salomon, F, Goiran, J-P, Bravard, J-P et al. (2014) A Harbour–Canal at Portus: A

- 1149 Geoarchaeological Approach to the Canale Romano: Tiber Delta, Italy. *Water History*
1150 6: 31-49.
- 1151 Salomon F, Keay S, Carayon N, et al. (2016) The Development and Characteristics of
1152 Ancient Harbours—Applying the PADM Chart to the Case Studies of Ostia and
1153 Portus. *PLoS ONE* 11(9).
- 1154 Salomon F, Goiran J-P, Pannuzi S, et al. (2017) Long-Term Interactions between the Roman
1155 City of Ostia and Its Paleomeander, Tiber Delta, Italy. *Geoarchaeology* 32(2): 215–
1156 229.
- 1157 Salomon F, Goiran J-P, Noirot B, et al. (2018) Geoarchaeology of the Roman port-city of
1158 Ostia: fluvio-coastal mobility, urban development and resilience. *Earth-Science*
1159 *Reviews* 177: 265–283.
- 1160 Salomon F. (2020) Les origines d’Ostie : quelles interactions avec la dynamique
1161 d’embouchure ? (Delta du Tibre, Italie), *Archimède. Archéologie et histoire ancienne*
1162 7: 129-140
- 1163 Shanmugam, G., 2012. Process-sedimentological challenges in distinguishing paleo-tsunami
1164 deposits. *Nat Hazards* 63, 5–30.
- 1165
1166 Stock F, Knipping M, Pint A, et al. (2016) Human impact on Holocene sediment dynamics in
1167 the Eastern Mediterranean – the example of the Roman harbour of Ephesus. *Earth*
1168 *Surface Processes and Landforms* 41: 980–996.
- 1169 Strabo (1924) *Geography*. Loeb Classical Library. Cambridge.
- 1170 Tacitus (2010) *Annales*. Collection Des Universités de France. Paris: Les Belles lettres.
- 1171 Tinti, S. (1991) Assessment of tsunami hazard in the Italian seas. *Nat Hazards* 4: 267–283.
1172
- 1173 Tinti, S, Maramai, A and Graziani, L (2004) The New Catalogue of Italian Tsunamis. *Natural*
1174 *Hazards* 33: 439-65.
- 1175 Tortora P (1999) Modelli di distribuzione granulometrica sui fondali marini attraverso la
1176 Trend Surface Analysis, *Geologica Romana* 35 : 199–209.
- 1177 Tentori D, Milli S, Marsaglia KM (2018) A source-to-sink compositional model of a present
1178 highstand: an example in the low-rank Tiber depositional sequence (TDS) (Latium
1179 Tyrrhenian margin, Italy). *Journal of Sedimentary Research* 88: 1238–1259.
- 1180 Vött A, Fischer P, Hadler H et al. (2015) Detection of two different harbour generations at
1181 ancient Ostia (Italy) by means of geophysical and stratigraphical methods. In: Von
1182 Carnap-Bornheim C, Daim F, Ettl P et al. (eds) Häfen im 1. Millennium A.D.
1183 Bauliche Konzepte, herrschaftliche und religiöse Einflüsse. Interdisziplinäre
1184 Forschungen zu Häfen Von der Römischen Kaiserzeit bis zum Mittelalter.
1185 Regensburg: Schnell & Steiner, 23–34.
- 1186 Vött, A., Willershäuser, T., Hadler, H., Obrocki, L., Fischer, P., Heinzelmann, M. (2020).
1187 Geoarchaeological evidence of Ostia’s river harbour operating until the fourth century
1188 AD. *Archaeological and Anthropological Sciences* 12 : 26 p.

- 1189 Wang, Wang (1992). « Distribution of foraminifera in estuarine deposits: a comparison
1190 between Asia, Europe and Australia ». In *Centenary of Japanese micropaleontology*,
1191 71–83. Terra Scientific Publishing Tokyo.
- 1192 Wang, Pinxian, and John Chappell (2001). « Foraminifera as Holocene Environmental
1193 Indicators in the South Alligator River, Northern Australia ». *Quaternary*
1194 *International*, Australian Quaternary Studies: A Tribute to Jim Bowler, 83-85: 47-62.
- 1195 Wunderlich T, Wilken D, Erkul E, et al. (2018) The river harbour of Ostia Antica -
1196 stratigraphy, extent and harbour infrastructure from combined geophysical
1197 measurements and drillings. *Quaternary International* 473 (15): 55-65

1198
1199

1200 **Figures captions**

1201 **Figure 1.** Location map of the ancient harbour basin of Ostia and the palaeochannel of the
1202 Tiber (called *Fiume Morto*), and the sediment cores reviewed in this work.

1203 **Figure 2.** Synthesis of the palaeoenvironmental data from Core OST-3 redraw from Hadler et
1204 al. (2015).

1205 **Figure 3. (A)** Factor analysis of elemental concentrations in the Core PO-2. The number of
1206 factors is limited to four: (1) silicate detrital fraction (47%), (2) aluminosilicate detrital
1207 fraction vs carbonate fraction (13%), (3) anoxic conditions (10%), (4) seawater influence vs
1208 polluted freshwater (7%). **(B)** Distribution of factors with depth in the column able to identify
1209 the palaeoenvironments. The red shadings show the sedimentary deposits interpreted as
1210 tsunamis-related HEE-1 and 3 by Hadler et al. (2015). The highest Pb level palaeopollutions
1211 (see Delile et al., 2017 for details) recorded in the B2 unit strongly reject the assumption of a
1212 tsunami deposit for the HEE-3 (modified from Delile et al., 2018).

1213 **Figure 4.** Synthesis of the palaeoenvironmental data from Core OST-7A redraw from Vött et
1214 al. (2020).

1215 **Figure 5.** Synthesis of the palaeoenvironmental data from Core TEV-1A redraw from Hadler
1216 et al. (2020).

1217 **Figure 6.** Synthesis of the palaeoenvironmental data from Core TEV-4A redraw from Hadler
1218 et al. (2020).

1219 **Figure 7.** Plot of radiocarbon (2σ confidence range) and archaeological dates used by Hadler
1220 et al. (2015) and Vött et al. (2020) to define the tsunamis chronology of the ancient harbour
1221 basin of Ostia. To test this chronology, dates are compared with the depths of the four HEE
1222 layers (yellow boxes) and their chronological range (grey shadings) according to the current
1223 sea level. The red shading shows the depth of the only coarse layer (HEE-3) recorded in all
1224 the cores, and for which the bottom and upper limits are reported.

1225 **Figure 8.** Conceptual model of the recording of heavy metal palaeopollutions in the ancient
1226 harbour basins before, during, and after a palaeotsunami event.

1227 **Figure 9.** Main discussion points regarding the interpretation of the HEE units (See Table 1
1228 for more detailed discussion of the different indicators).

1229 **Table 1.** – Reviews of the evidences available for the seven high energy events identified in
1230 Hadler et al. (2015, 2020) and Vött et al. (2020).

12° 16' 33.60"E

12° 16' 55.20"E

12° 17' 16.80"E

12° 17' 38.40"E

12° 18' 0.00"E



Current channel of the Tiber River

PALAEOMEANDER OF OSTIA
IN 1557
(Fiume Morto)

TEV-1A

Hadler et al., 2020

TEV-4A

OSTIA
(Archaeological site)

HARBOUR OF OSTIA

OST-8
PO-2
PO-1
OST-6
OST-7A
OST-1 and 2
OST-3
OST-4

Coastline (ca. 2nd c. AD?)

500 m

- Main cores of this review
- Harbour of Ostia**
 - Cores from Goiran et al., 2014; Sadori et al., 2016; and Delile et al., 2018
 - Cores from Hadler et al., 2015; Vött et al., 2020
- Palaeomeander of Ostia**
 - Cores from Salomon et al., 2017; Pepe et al. 2016
 - Cores from Hadler et al., 2020

12° 16' 33.60"E

12° 16' 55.20"E

12° 17' 16.80"E

12° 17' 38.40"E

12° 18' 0.00"E

41° 45' 36.00"N

41° 45' 14.40"N

41° 45' 36.00"N

41° 45' 14.40"N

HARBOUR OF OSTIA / CORE OST-3

Foraminifers assemblage

Species density

Hypothesised High Energy Events do not show highest or lowest species diversity. Changes are abrupt for HEE-I and II.

Quantity

Selected dominant species (except reworked planktonic species)
Species reflect different estuarine environments.

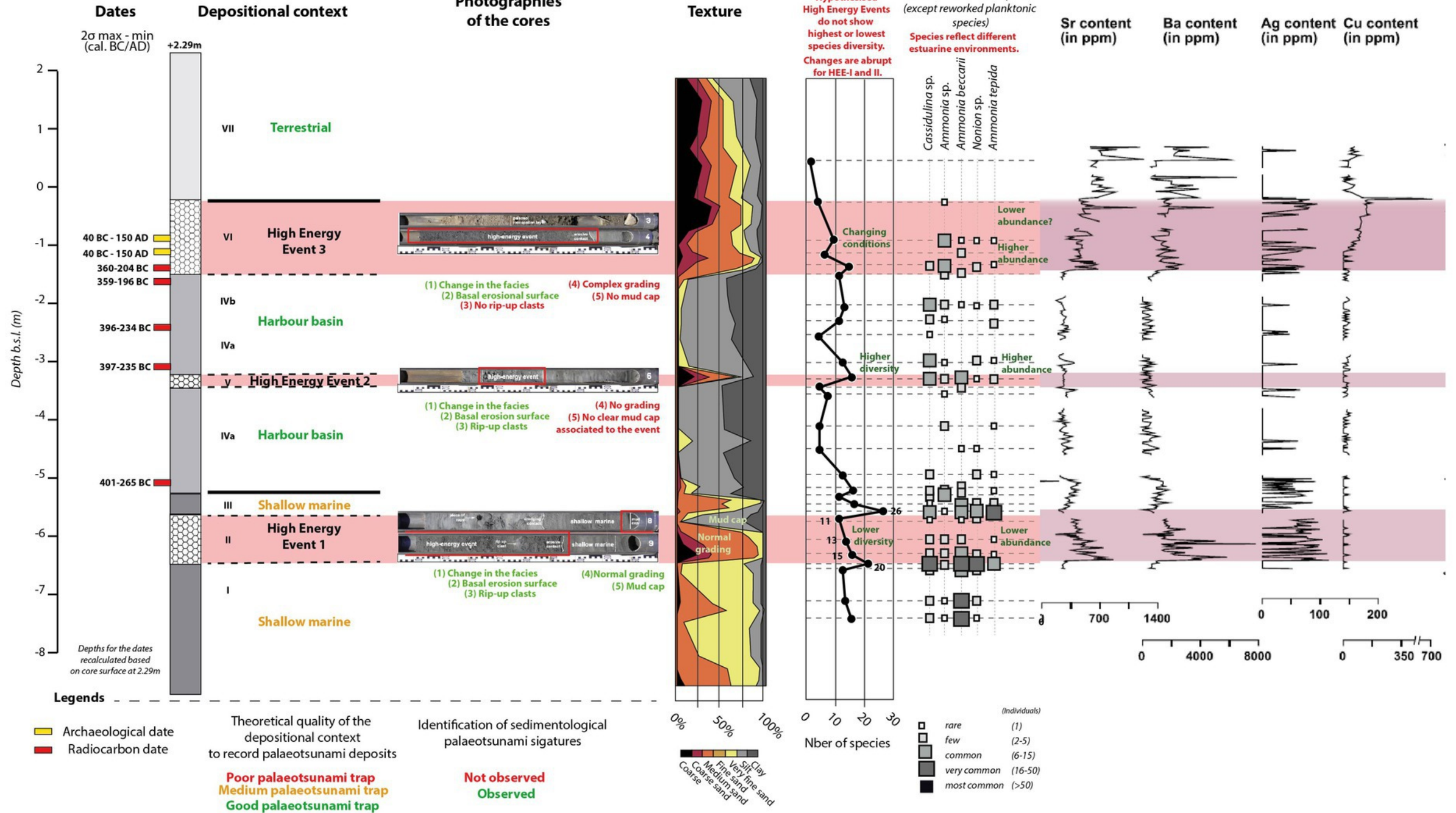
Geochemical indicators

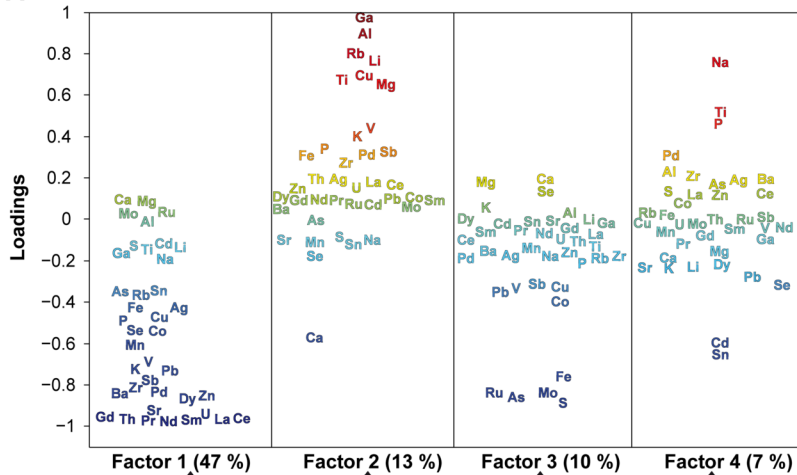
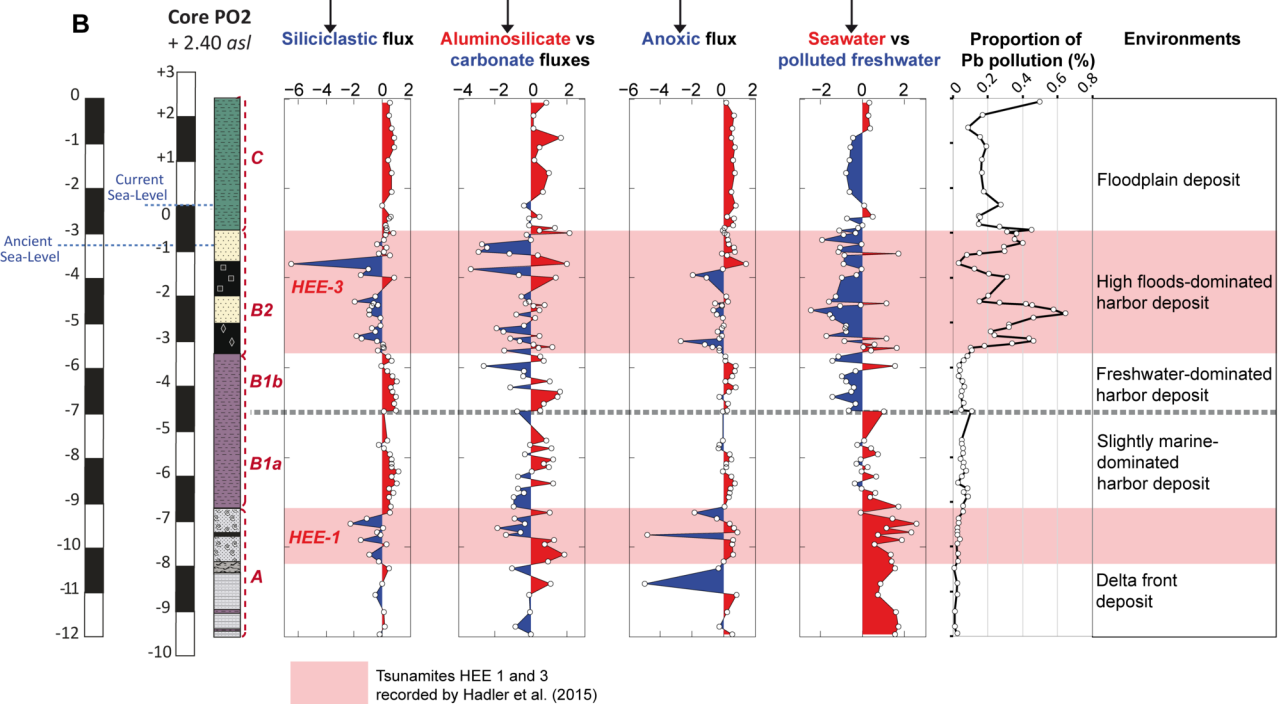
Sr content (in ppm)

Ba content (in ppm)

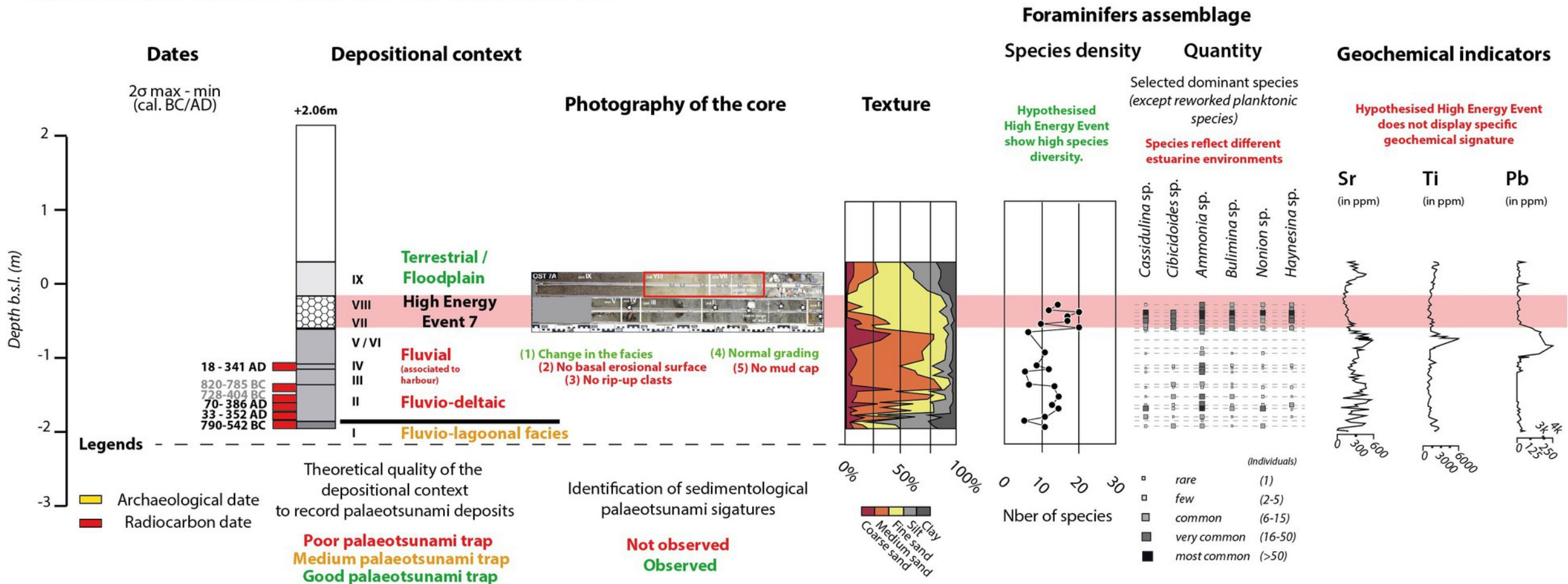
Ag content (in ppm)

Cu content (in ppm)



A**B**

HARBOUR OF OSTIA - SHIPSHED / CORE OST-7A

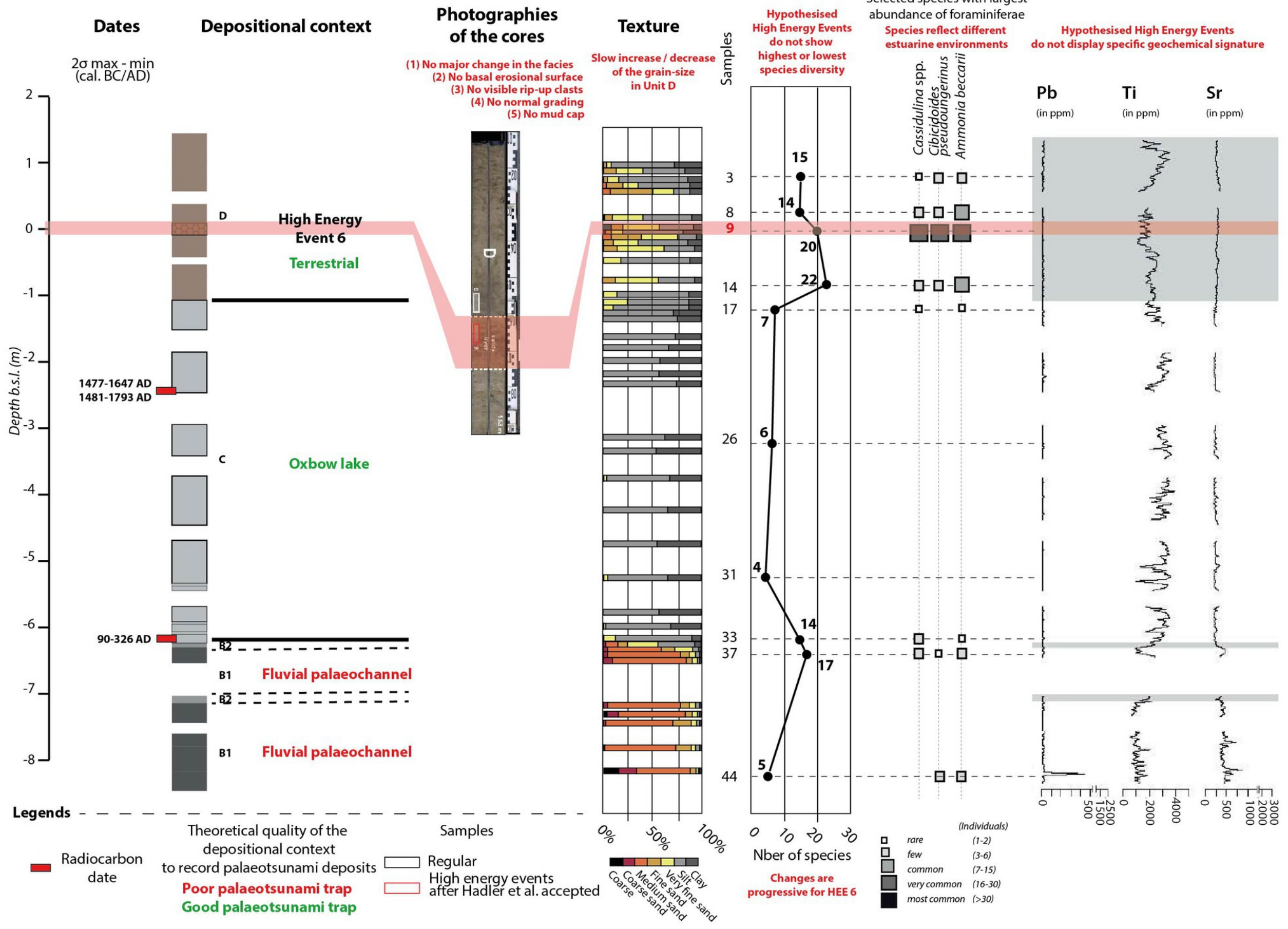


PALAEOMEANDER OF OSTIA / CORE TEV-1A

Foraminifera assemblage

Species density Quantity

Geochemical indicators



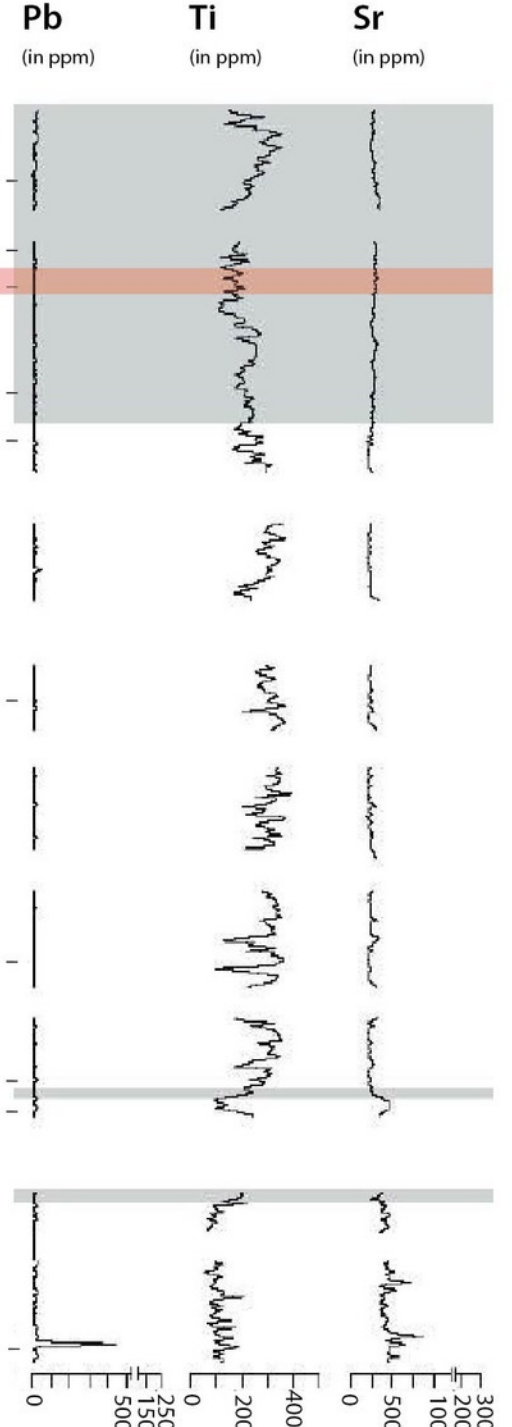
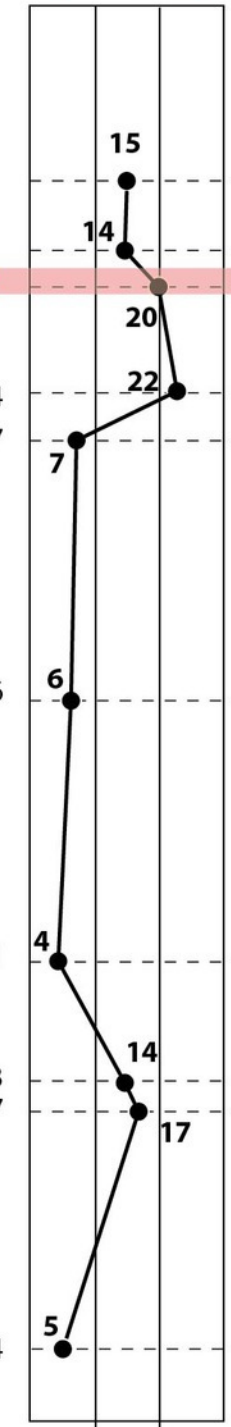
Hypothesised High Energy Events do not show highest or lowest species diversity

Selected species with largest abundance of foraminiferae reflect different estuarine environments

Hypothesised High Energy Events do not display specific geochemical signature

- Cassidulina spp.
- Cibicides pseudoungerinus
- Ammonia beccarii

Samples



Depth b.s.l. (m)

1477-1647 AD
1481-1793 AD

90-326 AD

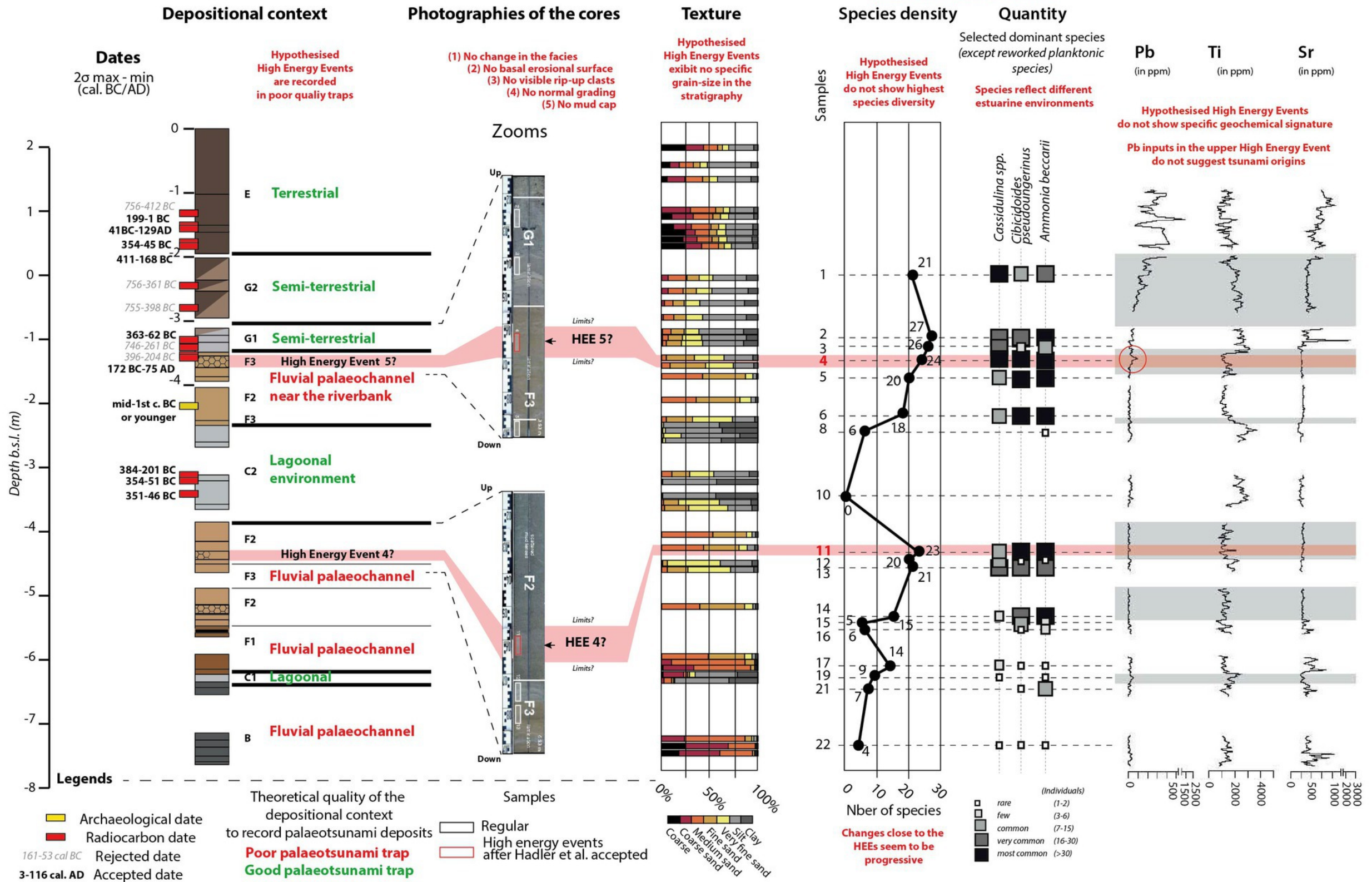
Theoretical quality of the depositional context to record palaeotsunami deposits
Poor palaeotsunami trap
Good palaeotsunami trap

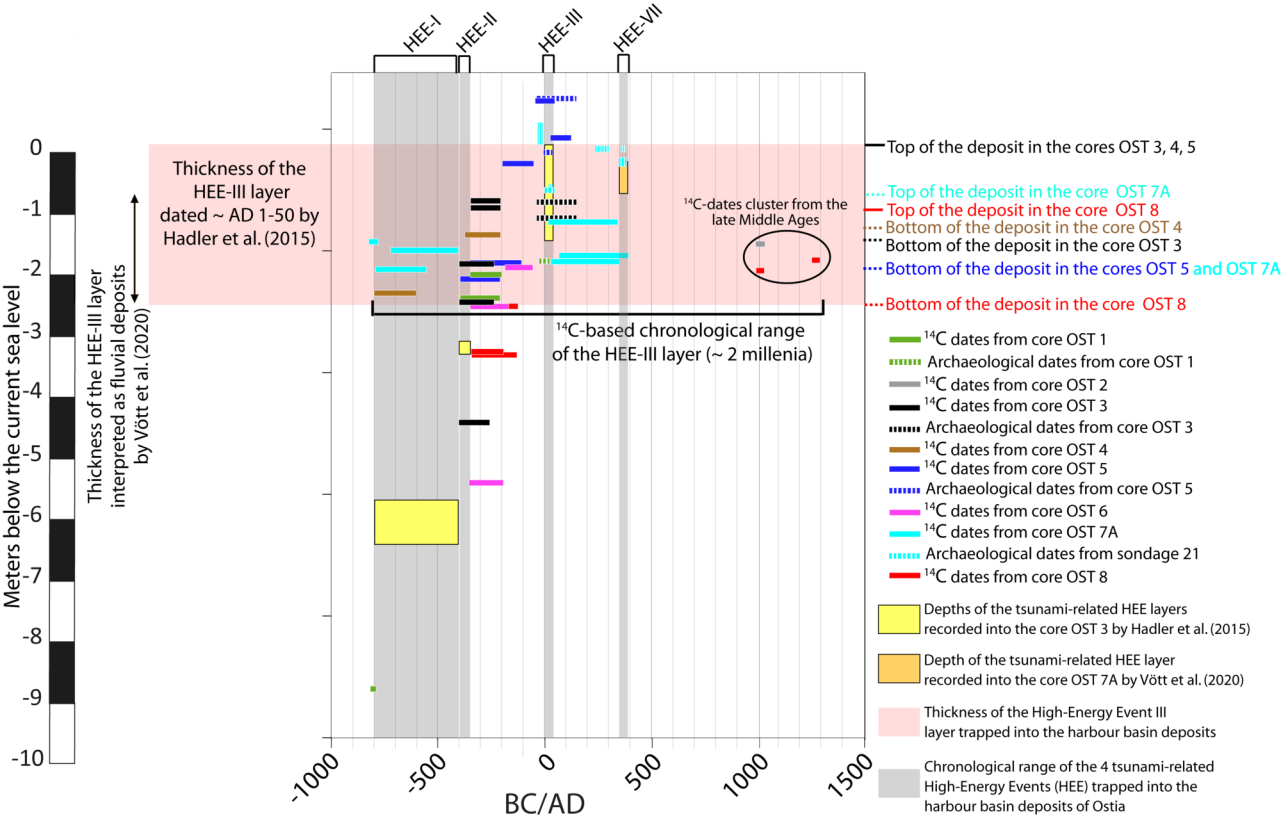
Samples
Regular
High energy events after Hadler et al. accepted

0% 50% 100%
Coarse sand
Medium sand
Fine sand
Very fine sand
Silt
Clay

(Individuals)
rare (1-2)
few (3-6)
common (7-15)
very common (16-30)
most common (>30)

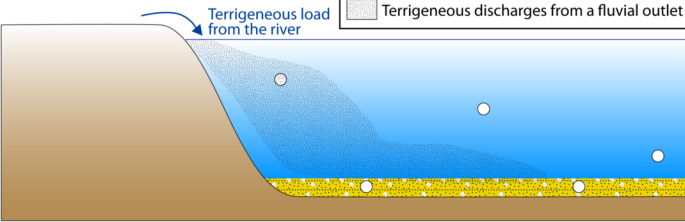
PALAEOMEANDER OF OSTIA / CORE TEV-4A



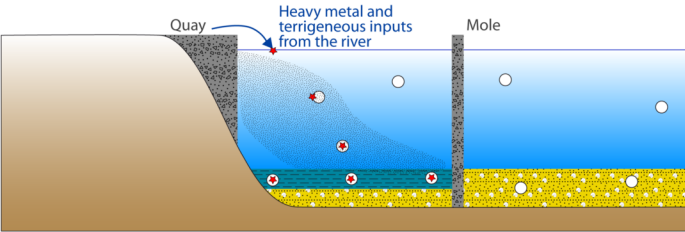


- Seawater components (flocculating cations; e.g. Ca^{2+} , Na^+ , etc.)
- ★ Lead, heavy metals (metallic cations; e.g. Pb^{2+} , Sn^{2+} , Zn^{2+} , Cu^{2+} , etc.)
- ⊙ Organo-mineral aggregates
- Holocene uncontaminated marine sands
- Graeco-Roman contaminated harbour muds
- Terrigenous discharges from a fluvial outlet

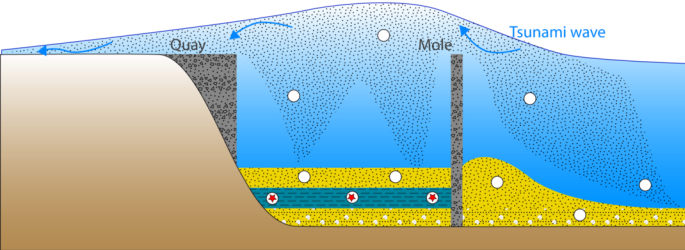
Stage 1: Pre-harbour environment



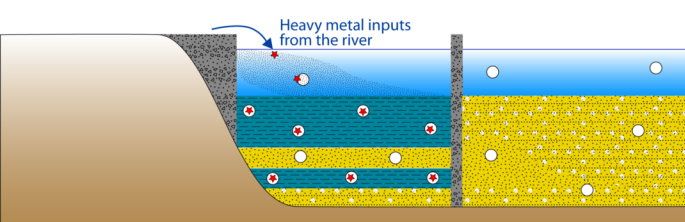
Stage 2: Functionnal harbour environment



Stage 3: Harbour environment disturbed by a tsunami inundation



Stage 4: Return to a functionnal harbour environment



TSUNAMI HYPOTHESES

(Hadler et al., 2015, 2020; Vött et al., 2020)

HYPOTHESES

CONSIDERING THE COMPLEXITY OF THE RIVER MOUTH DEPOSITIONAL CONTEXTS

(This paper)

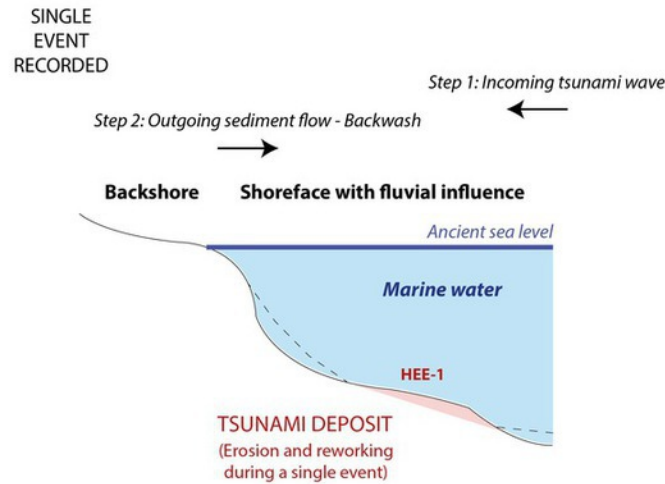
MAIN APPROACHES

- CHECK-LIST OF THE PALAEOTSUNAMI DEPOSIT INDICATORS CONSIDERED CONVINCING (see Table 1);
- POOR CONSIDERATION ABOUT THE COMPLEXITY OF THE RIVER MOUTH ENVIRONMENTS.

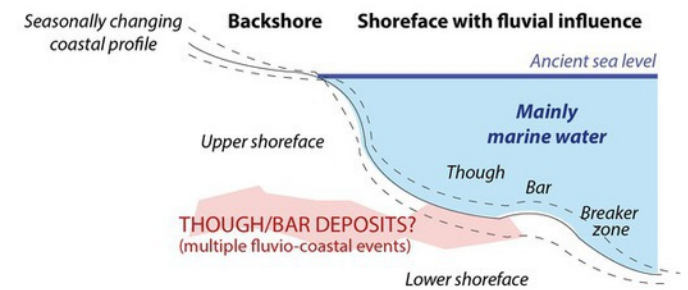
- CHECK-LIST OF THE PALAEOTSUNAMI DEPOSIT INDICATORS CONSIDERED NOT CONVINCING (many HEE deposits identified record few tsunami deposit characteristics - see Table 1);
- IMPORTANCE OF THE DEPOSITIONAL CONTEXT - RIVER MOUTH:
 - DYNAMIC RIVER MOUTH ENVIRONMENTS ARE NOT IDEAL FOR TRAPPING SINGLE HEE;
 - SALT WEDGE POSSIBLY EXPLAIN AUTOCHTHONOUS FORAMINIFERS DEVELOPMENT;
 - DIVERSITY OF THE TRANSPORT PROCESSES OF ALLOCHTHONOUS FORAMINIFERS SHOULD BE EXPLORED IN MORE DETAILS IN RIVER MOUTH CONTEXT (floating, reworking, flood/storm/tsunami transport);
- Pb POLLUTANT SHOULD ALSO BE USED FOR TESTING PALAEOTSUNAMI HYPOTHESES:
 - HIGH Pb CONCENTRATIONS COULD BE RECORDED IN ANCIENT FLOOD DEPOSITS, BUT WOULD BE MORE DILUTED IN REWORKED COASTAL SEDIMENTS.

PALAEO-COAST NEAR THE RIVER MOUTH

Interpretations for HEE-1

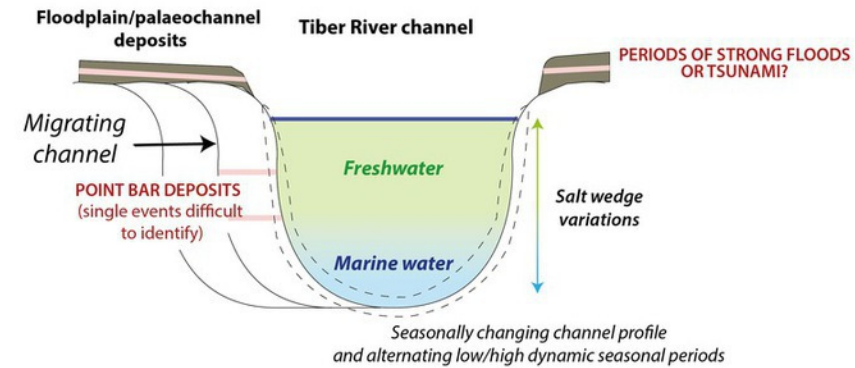
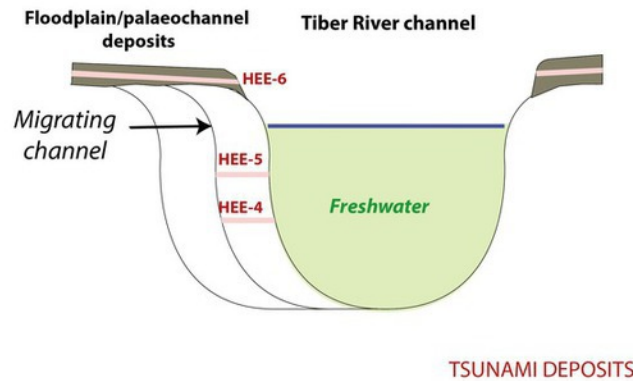


MULTI-EVENTS RECORDED
(Storms and floods seasonally recorded and possibly tsunamis)

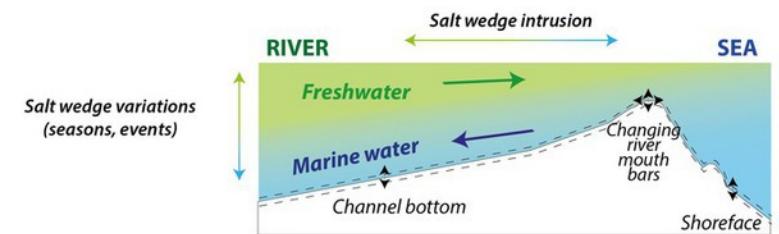


PALAEO-CHANNEL NEAR THE RIVER MOUTH

Interpretations for HEE-4, 5, 6

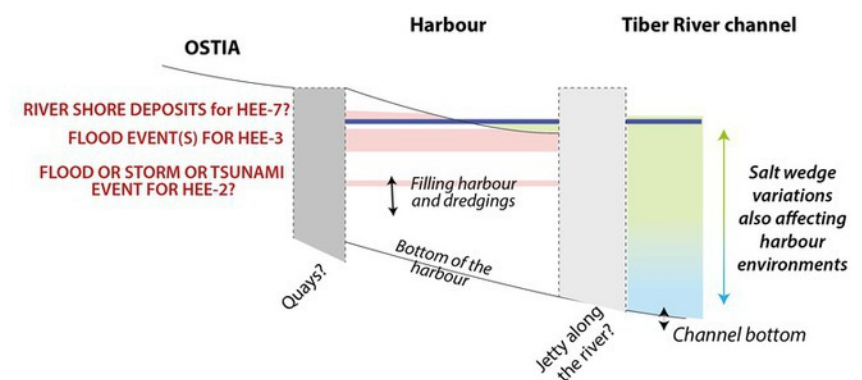
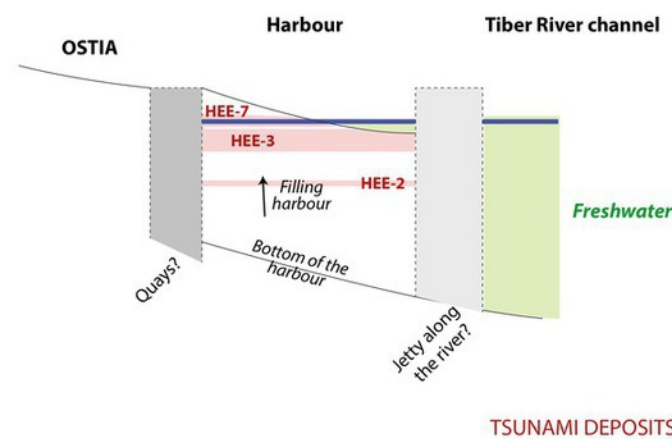


MOST LIKELY FLOOD DEPOSITS



ANCIENT HARBOUR NEAR THE RIVER MOUTH

Interpretations for HEE-2, 3, and 7



MULTIPLE HYPOTHESES COULD EXPLAIN COARSE MATERIAL DEPOSITION IN THE HARBOUR BASIN OF OSTIA

TYPES OF RIVER MOUTH ENVIRONMENTS

Higher	Higher ²⁴	- ²⁵	No clear specific assemblage ²⁶	No Gastropoda ²⁷	-	No ostracods ²⁸	Low Sr, Ti, MS ²⁹	Low	-	-	-	Possibly triggered by the AD 365 Crete earthquake (?)	Beach/riverbank close to the river mouth
Nothing specific in the context ³⁵	Higher ³⁶	Good ³⁷	No clear specific assemblage ³⁸	Shallow marine and estuarine species ³⁹	Articulate d state ⁴⁰	Articulated brackish ostracods ⁴¹	Nothing specific in the context	No	-	-	-	Tsunamigenic deposit ⁴²	Point bar fluvial deposit in estuarine environment

minated silt and sand document the (re-) establishment of medium-energetic conditions“ (Hadler et al. 2015, p84);

sp., Bulimina sp. and Brizalina sp. reflecting the local autochthonous marine to shallow marine environment“ (Hadler et al. 2015, p82);

ch facies I re-occur in high abundance. Additional groups like *Rosalina sp., Miliolinella sp. or Planorbulina sp.* And the increased content of *Posidonia* document the (re-) establishment of a shallow

er et al. 2015);

n “incorporated rip-up clasts”. “A fining upward sequence with a mud cap attests initially strong but subsequently decreasing flow dynamics” (Hadler et al. 2015, p82);

n the hinterland of the Tiber (Bellotti et al., 2007) » (Hadler et al. 2015, p82) > No data about the other foraminifers;

major environmental interruption associated with the high-energy deposit” (p82); “Recent planktonic foraminifera like *Orbulina sp.* and marine groups like *Ammonia sp. or Cassidulina sp.* clearly *Orbulina sp. Hyaline sp.* differs from shallow coastal environments below and above the HEE 1, but present in very small quantities. After Hadler et al. 2015 concerning HEE 1: « Recent planktonic

erals also seem to reflect the fingerprint of the Tiber river catchment that is dominated by volcanic rocks and Plio-/Pleistocene calcareous marine deposits (Bozzano et al., 2000; Bellotti et al.,

. 2015, p84);

ty and the occurrence of groups like *Ammonia sp. and Haynesina sp.*, tolerant to ecological stress, correspond well to unfavourable, brackish to freshwater environmental conditions typical of eae occur, probably related to variations in freshwater and seawater inflow” (Hadler et al. 2015, p84);

r basin” (Hadler et al. 2015, p84);

rey sand that incorporates cultural debris like ceramic fragments and a lead sheet”;

ud cap described;

deposits of the lagoonal harbour [in OST 6] are also overlain by a massive layer of sand including rip-up clasts and ceramic fragments.” (Hadler et al. 2015, p84) – No grading and no mud cap

re foraminifera with increasing abundances within the high-energy deposit while *Ostracodae* completely disappeared” (Hadler et al. 2015, p84);

ii, Cassidulina sp., Elphidium sp. or Orbulina sp. attesting the short-term input of sea-borne allochthonous sediments into the lagoonal harbour » (Hadler et al. 2015, p84).. > Additional work on the ally, no specific species were found for this HEE 2 comparing to the species commonly found in the lagoonal harbour of Ostia, below and above this unit;

es sp. may originate Gyroidinoides sp., Melonis sp. or Cibicidoides sp. may originate from slightly deeper marine environments» (Hadler et al. 2015, p84).. > Additional work on the current river *eloculina sp. and Nodosaria sp.* not observed in the lagoonal harbour but in very low density. Otherwise, all species are observed in the harbour sediments;

4);

in abundance in units VII and VIII” (Vött et al. 2020, p14 and 15 of 26);

man impact. The latter seems clearly associated with the use of the site as river harbour.” (Vött et al. 2020, p17 of 26);

n units VII and VIII (Fig. 8f, g) can be clearly seen.” (Vött et al. 2020, p13 of 26) ; No basal unconformity and rip up clasts evidences are reported;

s found here is up to double as high as in the sediments below” (Vött et al. 2020, p14 of 26) > A comparison with other cores analysed by the same research team would have been interesting. For

